1983ApJS...52..121G

THE ASTROPHYSICAL JOURNAL SUPPLEMENT SERIES, 52:121-153, 1983 June
© 1983. The American Astronomical Society. All rights reserved. Printed in U.S.A.

STELLAR SPECTROPHOTOMETRIC ATLAS, $3130 < \lambda < 10800$ Å[1]

JAMES E. GUNN
Palomar Observatory, California Institute of Technology, and Princeton University Observatory
AND
L. L. STRYKER
Yale University Observatory, and Dominion Astrophysical Observatory, Herzberg Institute of Astrophysics
Received 1981 October 16; accepted 1982 November 5

ABSTRACT

A spectrophotometric catalog of 175 stars covering a complete range of spectral types and luminosity classes is presented. The Oke multichannel scanner was used to obtain the energy distributions over the wavelength region $3130 < \lambda < 10800$ Å. Broad-band and Strömgren colors are computed from the scanner data, and these are compared with published photoelectric observations. The catalog is available on magnetic tape.

Subject heading: spectrophotometry

I. INTRODUCTION

Over the course of the past 10 years, a large body of homogeneous spectrophotometric data on relatively bright stars has been gathered to serve as a library with which to synthesize galaxy spectra in population studies (e.g., Gunn, Stryker, and Tinsley 1981). We have been persuaded that the catalog might be generally useful and have prepared the data to appear in this Supplement.

One hundred seventy-five (175) stars were selected, most from the Navy photometric catalog (Blanco *et al.* 1970), some of Eggen's (1967, 1969, 1971*a*, *b*) old disk moving groups, nearby clusters such as M67, Hyades, and Praesepe, and a few late-M variables from Kukarkin and Parenago (1954). Covered are complete ranges of spectral type and luminosity class.

The paper contains normalized spectral energy distributions of these stars in pictorial form, along with tables of calculated colors, scan line and continuum indices, and some information on how the scan colors are related to real photometric systems. The quality and treatment of the data reflect the intended purpose for which it was gathered, and may or may not suffice for other purposes; for example, the blue region in red stars and (especially) the red region in blue stars are often sufficiently noisy to mask any real features. This problem clearly does not affect a synthesis superposition which has contributions from both, but it may make the data less useful for some other purposes.

[1]Supported in part by NSF grants MPS73-04673, AST75-16329, AST77-23566, AST79-22012, AST80-23351, AST80-15346, and by Zonta International.

II. OBSERVATIONS AND REDUCTIONS

The observations were obtained with Oke's (1969) multichannel spectrophotometer at the Cassegrain focus of the 5 m Hale telescope. That instrument measures the entire range from 3000 to 12000 Å with two banks of photomultipliers, one looking at the second-order blue and the other the first-order red from a single grating. The spectral resolution is changed by inserting deckers in front of the photomultipliers to limit the length of spectrum transmitted in each channel. The grating is then moved in increments to fill in the resulting gaps in the spectrum. In the data presented here, the resolution is 20 Å in the blue and 40 Å in the red. To obtain critically sampled data, the grating was moved only half that spacing between data points; thus, there are points every 10 Å in the blue and 20 Å in the red. There were 21 settings per object with this scheme.

The spectrophotometer has a chopper whose primary purpose is to allow accurate sky subtraction on faint objects. The chopper was, in general, running when these observations were taken, although they were made with the object always in the same aperture. The sky corrections were quite small, even though the observations were mostly obtained in twilight. Coincidence corrections were applied to the pulse-counting rates, but these corrections were always less than 1%. The sky contribution was never more than 10% of the flux in any channel, and the aperture balance factors are known to much better than 10%; the resulting uncertainties in the fluxes are thus less than 1%.

The standards used are the faint Oke subdwarf standards HD 19445, 84967, 140283, and BD +17°4708. Halfway through the program it was realized that the

© American Astronomical Society • Provided by the NASA Astrophysics Data System

1983ApJS...52..121G

original calibrations were not sufficiently accurate in the 4000 Å region and near the Balmer lines. These deficiencies resulted in the "AB 79" recalibration to which these data have been reduced.

The AB 79 system is based on the composite Oke-Schild (1970)/Hayes-Latham (1975) fluxes as adopted in Hayes and Latham for α Lyr. The region of the high Balmer lines and Balmer jump were tied to scans of the hot subdwarfs BD +28°4211, Feige 34, and Feige 67. For these very hot stars the region is essentially featureless. These fluxes were then tied though an intermediate star [HD 196180: A3 V, $V = 4.6$, $B - V = 0.10$] to the primary faint standard BD +17°4708. Some smoothing was applied to the continuum calibration, particularly in the near-infrared, by using model atmospheres. The system is, in any case, essentially that of Hayes and Latham. A full discussion of the AB 79 calibration including details of the standard stars and the adopted absolute calibration of α Lyr appears in Oke and Gunn (1983).

One or two of these standards were observed every hour, and all cover the same air-mass range as the program stars, i.e., $\leqslant 1.5$. Data were reduced by using a standard extinction curve (Oke 1964). For each night, flux calibrations were found by a least-squares fit to the standards. Then, standard stars were reduced along with the program stars, and checks were made for systematic trends with time or air mass.

The practice used here of defining the instrumental response on a grid coarser than the one on which the observations were taken makes it impossible to remove localized telluric features such as the A band at 7600 Å and the highly variable water vapor bands at ~ 9400 Å without special observations, and no attempt was made to do this.

Most of the data were obtained under photometric conditions, but that for the early dwarfs and giants contain a subset taken through light cirrus. The result is variation from one grating setting to another of a few percent in the flux. This variation has been removed with the assumption that the absorption is gray, as is discussed further below, and the stars affected are so indicated in Table 1.

Some of the stars were too bright to be observed with the pulse-counting system in use and were observed either with the aid of an inconel "neutral" filter or with reduced telescope aperture. Generally, one or the other technique was necessary for stars brighter than about seventh magnitude. Nothing was assumed about the telescope response functions in these configurations, nor was it necessary to do so, since responses were measured and calibrated with standards during each night's usage. Since data for the brighter stars were treated in exactly the same way as those for the fainter stars, these stars are not explicitly identified in the tables.

A few instrumental quirks were evident in the raw data, the most serious being occasional systematic displacements of the points for a whole channel. This phenomenon was known to occur previously and is doubtless due to some mechanical instability in the spectrophotometer. Since the endpoints in each channel overlap at least one, and sometimes two, points with adjacent channels, correction of this particular ill is straightforward, although it may remain undetected if sufficiently small. Much more rarely a tilt appeared in data for some isolated channel. This was corrected in the same way if the correction was straightforward and appeared innocuous; otherwise, the data of that channel were discarded.

The raw energy distributions thus obtained were dereddened with a simple plane galactic extinction model, with the dust distributed vertically as $\mathrm{sech}\,(Z/70\ \mathrm{pc})$ and the visual absorption in the plane of 0.7 mag kpc^{-1}. (See the Appendix for the algorithms used to deredden the fluxes.) Absolute magnitudes as a function of spectral type were obtained from Blaauw (1963), and the distances calculated self-consistently with the absorption model. The monochromatic $A(\lambda)$ is the standard Whitford (1958) law. The absorption corrections are, in general, small, except for the early-type stars for which they are both larger and more critical. For a few of these cases the procedures fail markedly and have to be replaced by a different technique, described below.

Scans of the early-type stars (O–mid-A) showed two notable effects remaining at the end of the reduction process. First, a few scans obtained through light cirrus have spurious, cyclic features of small amplitude, due to slightly variable extinction, superposed upon them, plus some noise near 5760 Å, where the red and blue photomultipliers overlap. Second, the continuum slopes of a few stars were clearly at odds with those expected for their spectral type and size of Balmer jump. That is, it appears that the original reddening correction had been either too large or too small.

To remove the cycles, we used the normally featureless region between Hα and Hβ to note the periodicity. Then we fitted straight lines, one each for the red and blue sides, through a few cycles to determine the set of magnitude differences which defined the cycles. These magnitude errors were then subtracted over the entire stellar scan and the conversion made to corrected fluxes. This procedure assumes that the cirrus extinction is gray, which is an adequate approximation for the amplitudes involved (Serkowski 1970). Near 5760 Å we simply defined the continuum as the linear fit through the noise. Scans processed thus are listed with a "C" in the final column of Table 1.

To correct the failure of the original dereddening algorithm to deal properly with some of the early-type stars, we forced the problem stars to lie on the normal

© American Astronomical Society • Provided by the NASA Astrophysics Data System

© American Astronomical Society • Provided by the NASA Astrophysics Data System

1983ApJS...52..121G

TABLE 1

SCAN STARS, MAGNITUDES, AND COLORS

ID	STAR NAME	SP T	AV[a]	V	U-B	B-V	V-R	R-I	CODE
1	9 SGR	O5	1.12	4.8	-1.15	-0.34	-0.40	-0.44	CR
2	9 SGE	O8F	1.01	5.3	-1.11	-0.32	-0.38	-0.47	CR
3	HR 8023	O6	1.14	4.8	-1.08	-0.31	-0.39	-0.47	CR
4	-1 935	B1V	0.22	5.0	-0.95	-0.26	-0.34	-0.40	
5	60 CYG	B1V	0.17	5.3	-0.91	-0.27	-0.37	-0.44	CR
6	102 HER	B2V	0.25	4.1	-0.83	-0.25	-0.36	-0.45	CR
7	ETA HYA	B3V	0.03	4.1	-0.68	-0.20	-0.31	-0.35	R
8	IOTA HER	B3V	0.08	3.7	-0.67	-0.20	-0.32	-0.38	C
9	HR 7899	B4V	0.07	5.8	-0.65	-0.19	-0.34	-0.39	R
10	38 OPH	A1V	0.51	5.4	-0.49	-0.14	-0.29	-0.33	R
11	HR 7174	B6V	*0.06	6.0	-0.29	-0.11	-0.25	-0.31	R
12	9 VUL	B7V	*0.08	5.2	-0.28	-0.10	-0.25	-0.27	CR
13	HD 189689	B9V	0.09	7.2	-0.23	-0.08	-0.25	-0.25	
14	THETA VIR	A0V	0.03	4.3	0.15	-0.03	-0.21	-0.22	C
15	NU CAP	B9V	*0.06	4.8	0.05	-0.02	-0.21	-0.21	CR
16	HR 6169	A2V	0.07	6.4	0.18	-0.02	-0.20	-0.25	
17	HD 190849A	A1V	0.30	6.8	0.11	0.01	-0.22	-0.22	
18	69 HER	A2V	0.03	4.6	0.17	0.00	-0.20	-0.23	C
19	HD 190849B	A3V	0.30	7.3	0.18	0.06	-0.19	-0.20	
20	58 AQL	A0V	0.06	5.5	0.19	0.06	-0.17	-0.17	
21	78 HER	B9V	*0.29[b]	6.0	0.22	0.04	-0.17	-0.19	R
22	HR 6570	A7V	0.04	6.0	0.26	0.11	-0.17	-0.21	
23	HD 187754	A2V	0.11	8.4	0.34	0.13	-0.13	-0.11	
24	THETA1 SER	A5V	0.03	4.6	0.22	0.14	-0.12	-0.15	
25	PRAESEPE 276		0.01	7.6	0.32	0.16	-0.09	-0.13	C
26	PRAESEPE 114		0.01	8.2	0.25	0.17	-0.07	-0.12	
27	PRAESEPE 154		0.09	8.4	0.21	0.22	-0.06	-0.09	
28	HD 190192	A5V	0.16	8.5	0.22	0.23	-0.05	-0.08	
29	PRAESEPE 226		0.09	8.8	0.18	0.28	-0.01	-0.05	
30	PRAESEPE 37		0.09	8.9	0.16	0.31	0.01	-0.05	
31	HD 191177	F4V	0.10	8.7	0.22	0.31	0.04	-0.05	
32	PRAESEPE 332		0.09	9.6	0.08	0.39	0.07	-0.01	
33	BD+293891	F6V	0.09	9.1	0.11	0.40	0.10	0.00	
34	PRAESEPE 222		0.09	10.0	0.09	0.43	0.10	0.03	
35	HD 35296	F8V	0.01	4.8	0.10	0.49	0.16	0.06	
36	BD+263780	G0V	0.05	8.4	0.09	0.50	0.16	0.05	
37	HD 148816	F9V	0.03	7.3	-0.03	0.51	0.18	0.09	
38	HD 155675	F8V	0.05	8.4	0.04	0.51	0.19	0.09	
39	PRAESEPE 418		0.09	10.5	0.14	0.53	0.16	0.06	
40	HYAD 1		0.03	7.3	0.20	0.53	0.17	0.07	
41	HD 122693	F8V	0.04	8.0	0.21	0.51	0.19	0.04	
42	HD 154417	F8V	0.02	5.9	0.13	0.54	0.18	0.06	
43	HYAD 2		0.03	7.7	0.22	0.58	0.19	0.07	
44	HD 227547	G5V	0.06	9.8	0.23	0.59	0.20	0.09	
45	HD 154760	G2V	0.04	8.6	0.20	0.59	0.21	0.10	
46	HD 190605	G2V	0.03	7.6	0.28	0.59	0.20	0.08	
47	HYAD 15		0.03	8.0	0.28	0.62	0.22	0.10	
48	HD 139777A	K0V	0.01	6.6	0.20	0.63	0.24	0.09	
49	HD 136274	G8V	0.02	7.9	0.41	0.67	0.28	0.12	
50	HYAD 26		0.03	8.6	0.41	0.71	0.26	0.12	
51	HD 150205	G5V	0.02	7.5	0.38	0.70	0.26	0.14	
52	HYAD 21		0.03	9.1	0.54	0.77	0.28	0.15	
53	+02 3001	G8V	0.02	7.5	0.47	0.79	0.37	0.17	
54	HD 190571	G8V	0.02	7.4	0.59	0.82	0.34	0.20	
55	HYAD 183		0.03	9.6	0.78	0.89	0.39	0.22	
56	HD 190470	K3V	0.01	7.8	0.81	0.89	0.39	0.20	
57	HD 154712	K4V	0.02	8.6	0.99	0.97	0.49	0.27	
58	HYAD 185		0.03	9.4	1.00	1.07	0.55	0.34	
59	+38 2457	K8V	0.01	9.8	1.17	1.06	0.56	0.27	
60	HYAD 173		0.03	10.4	1.30	1.20	0.65	0.41	
61	GL 40	M0V	0.01	8.9	1.30	1.27	0.76	0.47	
62	HYAD 189		0.03	11.0	1.39	1.32	0.75	0.49	
63	HD 151288	K7V	0.01	8.0	1.34	1.35	0.76	0.50	
64	HD 157881	K7V	0.00	7.5	1.37	1.33	0.79	0.52	
65	BD 132683	M0V	0.01	9.4	1.38	1.34	0.83	0.52	
66	GL 15A	M0V	0.00	8.0	1.33	1.51	1.06	0.81	
67	GL 49	M2V	0.00	9.5	1.34	1.44	1.06	0.83	
68	GL 109	M4V	0.00	10.5	1.38	1.50	1.23	1.04	
69	GL 15B	M6V	0.00	11.0	1.57	1.71	1.46	1.22	
70	GL 83.1	M8V	0.00	12.2	1.45	1.70	1.67	1.40	
71	GL 65	M5V	0.01	12.0	1.22	1.77	2.08	1.74	
72	HR 7567	B1IV	0.64	5.1	-0.86	-0.25	-0.38	-0.44	CR
73	HR 7591	B2III	0.13	5.8	-0.84	-0.25	-0.34	-0.41	CR
74	20 AQL	B3IV	0.67	4.5	-0.54	-0.16	-0.31	-0.34	CR
75	HR 7467	B3III	0.13	6.5	-0.57	-0.18	-0.32	-0.37	CR
76	IOTA LYR	B7IV	0.03	5.4	-0.42	-0.13	-0.28	-0.31	CR
77	HR 7346	B7III	*0.05	6.4	-0.29	-0.11	-0.27	-0.30	CR
78	59 HER	A3III	0.07	5.4	0.20	-0.05	-0.24	-0.24	C
79	HR 6642	A0IV	0.09	6.0	0.07	-0.04	-0.25	-0.27	
80	11 SGE	B9IV	*0.04	5.8	0.03	-0.03	-0.23	-0.26	CR
81	60 HER	A3IV	0.04	4.8	0.23	0.09	-0.16	-0.19	C
82	HD 192285	A4IV	0.17	8.0	0.24	0.12	-0.14	-0.14	
83	ALPHA OPH	A5III	0.01	2.0	0.24	0.15	-0.11	-0.15	C
84	HD 165475B	A5IV	0.09	7.5	0.32	0.23	-0.08	-0.12	
85	HD 165475	A5IV	0.07	7.1	0.26	0.25	0.00	-0.03	
86	XI SER	F0IV	0.01	3.5	0.26	0.24	-0.04	-0.08	
87	HD 5132	F0IV	0.06	7.6	0.18	0.29	0.00	-0.08	
88	HD 508	A9IV	0.12	8.1	0.28	0.31	0.00	-0.05	
89	HD 210875	F0IV	0.15	8.5	0.30	0.32	-0.02	-0.05	
90	RHO CAP	F2IV	0.03	4.7	0.14	0.34	0.05	-0.02	

© American Astronomical Society • Provided by the NASA Astrophysics Data System

1983ApJS...52..121G

TABLE 1—*Continued*

ID	STAR NAME	SP T	AV	V	U-B	B-V	V-R	R-I	CODE
91	HD 7331	F7IV	0.08	7.2	0.13	0.43	0.08	0.00	
92	BD+630013	F5IV	0.16	8.7	0.10	0.44	0.08	0.01	
93	HD 13391	G2IV	0.09	8.5	0.18	0.55	0.19	0.05	
94	HD 154962	G8IV	0.03	6.2	0.37	0.64	0.23	0.11	
95	HD 192344	G4IV	0.06	7.7	0.37	0.65	0.22	0.11	
96	HR 6516	G6IV	0.02	5.3	0.38	0.65	0.22	0.08	
97	HR 7670	G6IV	0.03	5.7	0.48	0.67	0.23	0.08	
98	HD 128428	G3IV	0.05	7.6	0.50	0.71	0.26	0.12	
99	31 AQL	G8IV	0.02	5.1	0.48	0.73	0.27	0.09	
100	-02 4018	G5IV	0.08	8.6	0.58	0.79	0.35	0.15	
101	M67 F143?		0.14	11.2	0.62	0.81	0.34	0.16	
102	HD 11004	G5IV	0.07	8.0	0.53	0.82	0.39	0.24	
103	HD 173399A	G5IV	0.05	7.2	0.61	0.81	0.33	0.21	
104	HD 56176	G7IV	0.03	6.2	0.63	0.86	0.36	0.23	
105	HD 227693	G5IV	0.13	9.0	0.74	0.87	0.35	0.21	
106	HD 199580	K2IV	0.05	7.1	0.83	0.88	0.38	0.21	
107	HD 152306	G8III	0.09	6.9	0.69	0.88	0.35	0.17	
108	PRAESEPE 212		0.08	6.5	0.84	0.89	0.36	0.21	
109	THETA1 TAU	G8III	0.03	3.7	0.87	0.90	0.37	0.22	
110	HD 170527	G5IV	0.04	6.7	0.79	0.92	0.39	0.23	
111	HD 136366	K0III	0.07	6.1	0.93	0.93	0.37	0.24	
112	HD 191615	G8IV	0.06	7.7	0.89	0.95	0.42	0.26	
113	HD 124679	K0III	0.05	5.1	0.89	0.95	0.38	0.22	
114	HD 131111	K0III	0.05	5.3	0.94	0.96	0.43	0.28	
115	HD 113439	K0III	0.07	7.1	1.04	0.96	0.42	0.21	
116	HD 4744	G8IV	0.05	7.5	0.88	0.99	0.47	0.29	
117	HD 7010	K0IV	0.07	8.0	0.90	0.99	0.45	0.27	
118	46 L MI	K0III	0.03	3.7	1.03	0.99	0.45	0.26	
119	91 AQR	K0III	0.03	4.1	1.12	1.01	0.44	0.25	
120	M67 F141		0.14	10.2	1.14	1.01	0.43	0.23	
121	HR 8924A	K3III	0.07	6.1	1.25	1.01	0.42	0.23	
122	HD 140301	K0IV	0.03	6.3	1.16	1.02	0.44	0.28	
123	HD 95272	K0III	0.03	4.0	1.11	1.04	0.45	0.29	
124	HD 72184	K2III	0.06	5.7	1.25	1.05	0.43	0.27	
125	HD 119425	K2III	0.05	5.2	1.17	1.04	0.44	0.25	
126	HD 106760	K1III	0.04	4.9	1.20	1.07	0.47	0.28	
127	PSI U MA	K1III	0.02	2.9	1.24	1.08	0.48	0.29	
128	PHI SER	K1III	0.05	5.5	1.31	1.07	0.40	0.24	
129	HD 136514	K3III	0.06	5.3	1.44	1.11	0.46	0.29	
130	MU AQL	K3III	0.05	4.4	1.37	1.12	0.48	0.27	
131	HR 5227	K2IIIP	0.07	6.17	1.36	1.15	0.51	0.29	
132	HD 154759	K3III	0.12	8.09	1.41	1.17	0.54	0.29	
133	20 CYG	K3III	0.06	4.93	1.69	1.20	0.47	0.29	
134	ALPH SER	K2III	0.01	2.51	1.36	1.10	0.47	0.30	
135	MU LEO	K2III	0.03	3.73	1.52	1.17	0.52	0.30	
136	+1 3131	K0III	0.08	6.4	1.20	1.14	0.52	0.31	
137	M67 F170		0.14	9.4	1.66	1.24	0.58	0.34	
138	18 LIB A	K2IIIP	0.06	5.7	1.52	1.19	0.52	0.35	
139	+28 2165	K1IV	0.07	9.6	1.64	1.26	0.61	0.36	
140	NGC 188 1-69		0.10	12.2	1.54	1.23	0.57	0.38	
141	+30 2344	K3III	0.08	10.2	1.69	1.26	0.63	0.37	
142	HD 83618	K3III	0.04	3.7	1.55	1.26	0.60	0.39	
143	HD 158885	K3III	0.14	7.0	1.52	1.26	0.60	0.42	
144	HD 166780	K5III	0.14	7.2	1.79	1.32	0.65	0.42	
145	HD 148513	K4III	0.07	5.3	1.94	1.39	0.59	0.43	
146	M67 T626		0.14	9.1	1.86	1.39	0.67	0.43	
147	HD 127227	K5III	0.08	7.3	2.00	1.39	0.74	0.48	
148	M67 IV-202		0.15	8.5	2.07	1.46	0.78	0.51	
149	HD 50778	K4III	0.04	3.9	1.85	1.38	0.71	0.52	
150	HD 62721	K5III	0.07	4.7	1.87	1.39	0.73	0.53	
151	HD 116870	M0III	0.07	5.1	1.90	1.41	0.78	0.57	
152	HD 60522	M0III	0.05	3.8	2.04	1.48	0.80	0.60	
153	-1 3113	K5III	0.13	8.2	2.33	1.61	0.86	0.61	
154	+2 2884	K5III	0.09	6.6	2.05	1.43	0.84	0.63	
155	-2 3873	M0III	0.10	6.9	2.13	1.55	1.06	0.85	
156	HD 104216	M2III	0.10	6.0	1.93	1.52	1.04	0.87	
157	HD 142804	M1III	0.12	6.4	2.31	1.69	1.02	0.91	
158	HD 30959	M3III	0.06	4.5	2.14	1.71	1.30	1.06	
159	HD 151658	M2III	0.19	7.2	2.31	1.77	1.36	1.12	
160	-2 4025	M2III	0.12	8.8	2.04	1.64	1.42	1.20	
161	-01 3097	M2III	0.13	9.0	2.06	1.61	1.51	1.28	
162	TX DRA		0.11	7.1	1.88	1.55	1.52	1.34	
163	Z CYG	M8III	0.31	8.3	1.88	1.57	1.62	1.36	
164	+01 3133	M5III	0.12	8.9	1.71	1.50	1.77	1.51	
165	-2 3886	M5III	0.10	9.0	1.62	1.54	1.93	1.58	
166	W HER	M6III	0.12	10.6	0.82	1.10	2.56	1.96	
167	TY DRA	M8	0.14	8.8	1.27	1.56	2.35	1.97	
168	SW VIR	M7III	0.09	7.0	1.01	1.67	2.78	2.11	
169	RZ HER	M6III	0.31	12.8	0.13	1.38	3.07	2.40	
170	R LEO		0.11	8.9	0.31	1.92	3.67	2.79	
171	AW CYG	N	0.32	8.2	2.61	3.79	1.65	0.96	
172	WZ CAS	N	0.33	6.5	3.58	2.64	1.40	1.07	
173	69 CYG	B0IB	0.44	5.5	-1.03	-0.23	-0.37	-0.40	C
174	HR 7699	B5IB	1.05	5.2	-0.58	-0.19	-0.32	-0.38	C
175	HR 8020	B8IA	1.33	4.4	-0.55	0.03	-0.15	-0.20	C

[a] An * indicates a negative value for A_V.

[b] The large negative A_V indcates that the reddening is not well understood; this star should be used with caution.

1983ApJS...52..121G

(AQ3, Allen 1973) two-color relation in the $(U-B, B-V)$-plane, using the usual dereddening vector of slope 0.72, and obtained a new differential color excess, $\Delta E(B-V)$. The difference in visual absorption, $\Delta A_v = 3 * \Delta E(B-V)$, then enters into a wavelength-dependent magnitude correction of the form

$$m_{\rm corr}(\lambda) = \Delta A_v * [f(\lambda) - 1],$$

where $f(\lambda)$ is identical to that used in the original reduction. Fluxes were then recalculated from the corrected magnitudes. Colors were recalculated by passing broad-band filters (see below) through the fluxes. Scans processed in this manner are listed with an "R" in the final column of Table 1.

III. THE SCAN COLORS

The scans were convolved with standard U, B, V, R, and I response functions (UBV, Matthews and Sandage 1963; R, Sandage and Smith 1963; I, Johnson 1965) to obtain broad-band colors on standard systems. To check the scan colors for accuracy and reliability, we referred to Nicolet's (1978) collection of $U-B$ and $B-V$ observed data; for $R-I$ we searched the literature ourselves. For $U-B$ and $B-V$ we used *our* determined visual absorption to deredden Nicolet's values. Stars marked as doubles, variables, and ones with measurements having low weight were not included in the fits. Figure 1 shows these values plotted against the scan colors: open circles represent giants and filled circles dwarfs. We find tightly linear fits:

$$(U-B)_0 = -0.107 + 0.978(U-B)_{\rm scan} \quad \pm 0.044 \text{ (s.e.)} \quad (74),$$

$$(B-V)_0 = 0.009 + 1.030 * (B-V)_{\rm scan} \quad \pm 0.019 \quad (74),$$

$$-0.32 < (B-V)_{\rm scan} < 1.55$$

$$(R-I)_0 = 0.223 + 1.182 * (R-I)_{\rm scan} \quad \pm 0.031 \quad (50),$$

$$-0.08 < (R-I)_{\rm scan} < 0.65$$

where we have combined the fits for giants and dwarfs and the number in parentheses is the number of stars used in the fit. The redder giants are excluded since most are variable. The errors shown are the scatter in individual color data. Recall that R_0 comes from the Johnson R passband with effective wavelength ($\lambda_{\rm eff}$) of ~ 7000 Å, whereas $R_{\rm scan}$ is derived from the narrower Sandage and Smith (1963) r having $\lambda_{\rm eff}$ near 6500 Å. A zero-point shift is therefore not unexpected. The U filter begins at 3000 Å, and the I filter ends at 11500 Å, but the scan fluxes begin and end at 3160 and 10620 Å. This incomplete coverage is absorbed by the color terms in the transformation equations.

Following the discussion by Breger (1974, 1976), we calculated Stromgren *uvby* indices from our scans of B, A, and early F stars. Filter responses used were those of Crawford and Barnes (1970). The comparison with published, photoelectrically measured, *uvby* values (Hauck and Mermilliod 1980) is, again, quite adequate for most purposes. To convert scanner values into unreddened measured indices, the following relationships can be used:

$$(b-y)_0 = 0.182 + 0.917 * (b-y)_{\rm scan} \quad \pm 0.020 \quad (32),$$

$$(m_1)_0 = -0.045 + 1.135 * (m_1)_{\rm scan} \quad \pm 0.035 \quad (31),$$

$$(c_1)_0 = -0.198 + 0.997 * (c_1)_{\rm scan} \quad \pm 0.040 \quad (32),$$

$$(u-b)_0 = 0.153 + 0.919 * (u-b)_{\rm scan} \quad \pm 0.028 \quad (31).$$

In all cases, the reddenings used were those determined in the scanner reduction programs. The standard deviations for these data are clearly small and indicate very good internal and external consistency. In fact, these errors compare most favorably with residuals for other studies listed in Ardeberg and Virdefors (1980, Table II).

IV. DISCUSSION

Magnitudes and colors listed in Tables 1 and 2 and those supplied on the tape are in the dereddened scanner system. Table 3 lists colors transformed to the standard system.

Table 1 lists the stars in the atlas in $B-V$ order for those with $(B-V)_{\rm scan} < 1.10$ or in $R-I$ order for ones with $(R-I)_{\rm scan} > 0.35$. The first column is the identification number of the scan in order on the magnetic tape; the second is the star designation, usually HD number, or name; third is the spectral type and luminosity class information taken from the literature. The fourth and fifth columns are the visual absorption and V magnitude as calculated in the scan reductions mentioned in § II; sixth through ninth are the scan colors $U-B$, $B-V$, $V-R$, and $R-I$. The final column lists a code if the scan was further corrected: "C" for the cycling effects or "R" for reddening problems (see § II).

Table 2 lists the same stars with a number of continuum and feature indices. These were calculated from the scans themselves, without any smoothing, and, in some cases, i.e., those marked with a plus sign or "ST" (for Spinrad-Taylor), are similar to, but not identical with other commonly used indices. The first two columns are as above: column (1) gives the tape order number of the scan, column (2) is the stellar identification or name. The next seven columns are scan "con-

© American Astronomical Society • Provided by the NASA Astrophysics Data System

1983ApJS...52..121G

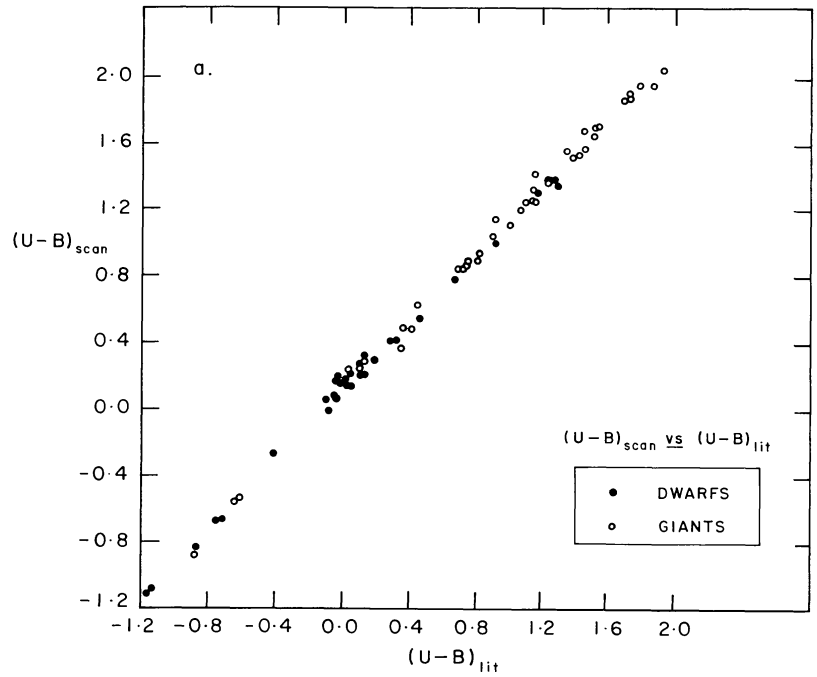

FIG. 1*a*

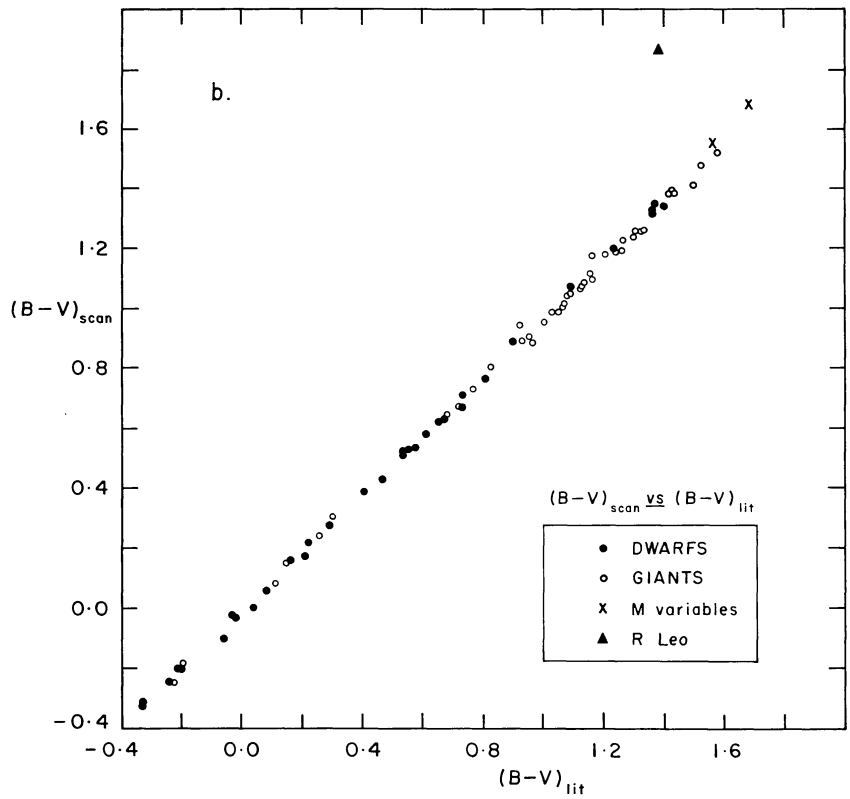

FIG. 1*b*

FIG. 1.—Scanner colors vs. measured broad-band colors on Johnson system. (*a*) $(U-B)_{\rm scan}$ vs. $(U-B)_{0,\rm pe}$; (*b*) $(B-V)_{\rm scan}$ vs. $(B-V)_{0,\rm pe}$.

© American Astronomical Society • Provided by the NASA Astrophysics Data System

1983ApJS...52..121G

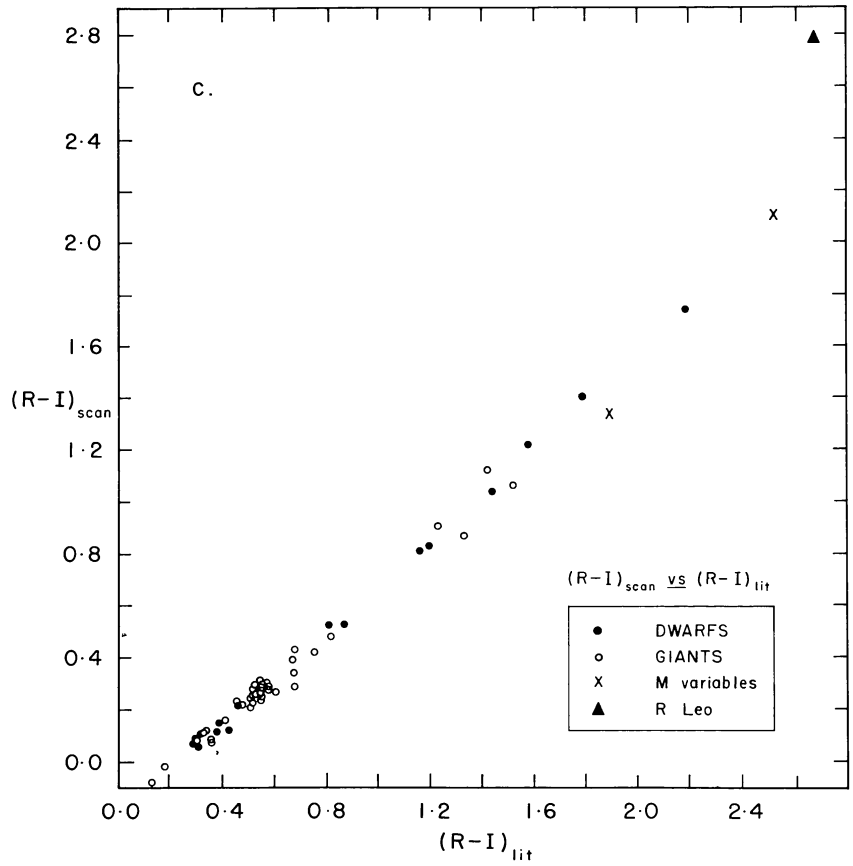

FIG. 1*c*.—$(R-I)_{\rm scan}$ vs. $(R-I)_{0,\rm pe}$.

tinuum" colors at approximate wavelengths (in 100 Å units): column (3) 33–37; column (4), 37–40; column (5), 40–46; column (6), 46–V, column (7), V–70; column (8), 70–87; and column (9), 87–99. Feature indices are the remaining 11 columns: column (10), Balmer break; column (11), CN 38+; column (12), 41–42; column (13), Ca H; column (14), Ca K; column (15), TI 61+; column (16), TI 71+; column (17), Ca 42; column (18), CH 43; column (19), Mg 51; and column (20), Na D.

Table 3 lists the star identification number and the dereddened colors, in the standard system, of $(U-B)_0$, $(B-V)_0$, and $(R-I)_0$.

Shown, in order, are dwarfs, Figure 2*a*–2*g*; giants, Figure 2*h*–2*r*; carbon stars, Figure 2*s*; supergiants, Figure 2*t*. Note the double scale on the abscissa; the upper is a logarithmic frequency scale, while the lower is a wavelength scale in units of 1000 Å. Tick marks on the ordinate represent 1 mag each. Scan fluxes are normalized such that the V magnitude equals zero.

The juxtaposition of scans in color order shows clearly the spectral changes with decreasing temperature. Also, stars with particularly strong or weak features relative to stars with similar colors are easily discernible. The feature indices listed in Table 2 provide another way to distinguish these stars when indices are consistently relatively strong or weak. Included in the atlas are some very strong lined K giants, some of which have been previously designated as "SMR" stars (Spinrad and Taylor 1969; Faber 1977). Most other stars represent the typical nearby old-disk population with a mean metallicity about one-half solar.

Should the reader wish to obtain the complete set of the multichannel scans in card-image format on magnetic tape, this may be accomplished by sending a blank 2400 ft tape to: Astronomical Data Center, National Space Science Data Center, Code 601, Greenbelt, MD 20771 USA; attention: Dr. W. H. Warren, Jr. Included in the tape are ID number; identification (name, spectral type); V, visual absorption; $U-B$, $B-V$, $V-R$, $R-I$ in scan system; sec Z, two plot delimiters, R.A., Decl., csc b; normalized fluxes at 509 wavelengths; flux error estimates; continuum and feature indices. Complete instructions for reading the tape will be provided.

The authors wish to thank Beatrice Tinsley and Gillian Knapp for constant encouragement and continual, but gentle, prodding. Thanks also to Benjamin Taylor and James Hesser for helpful suggestions.

© American Astronomical Society • Provided by the NASA Astrophysics Data System

© American Astronomical Society • Provided by the NASA Astrophysics Data System

1983ApJS...52..121G

TABLE 2

SCAN STARS AND ADDITIONAL INDICES

ID	NAME	SCAN "CONTINUUM" COLORS							FEATURE INDICES							ST			
		33-37	37-40	40-46	46-V	V-70	70-87	87-99	BREAK	CN38+	41-42	CA H	CA K	TI61+	TI71+	CA42	CH43	MG51	NA D
1	9 SGR	-0.22	-0.09	-0.23	-0.38	-0.48	-0.38	-0.27	-0.05	-0.03	-0.01	0.07	-0.01	0.05	0.02	0.04	0.01	0.15	0.03
2	9 SGE	-0.20	-0.07	-0.21	-0.39	-0.46	-0.45	-0.27	0.00	-0.03	-0.04	0.06	0.01	0.04	0.04	0.04	0.04	0.14	-0.01
3	HR 8023	-0.19	-0.02	-0.22	-0.37	-0.46	-0.47	-0.25	0.02	-0.04	-0.04	0.09	0.02	0.04	0.04	0.03	0.05	0.15	0.01
4	-1 935	-0.17	0.10	-0.21	-0.33	-0.40	-0.38	-0.17	0.01	0.01	-0.02	0.17	-0.05	0.06	0.04	0.02	0.04	0.14	0.01
5	60 CYG	-0.16	0.14	-0.18	-0.35	-0.44	-0.42	-0.22	0.01	0.01	-0.02	0.13	-0.01	0.04	0.02	0.02	0.05	0.13	0.01
6	102 HER	-0.20	0.26	-0.16	-0.34	-0.41	-0.43	-0.21	0.01	0.02	-0.04	0.18	0.00	0.04	0.04	0.04	0.05	0.14	0.00
7	ETA HYA	-0.11	0.35	-0.16	-0.30	-0.36	-0.33	-0.16	0.05	0.02	-0.01	0.21	-0.07	0.06	0.03	0.02	0.05	0.15	0.02
8	IOTA HER	-0.18	0.40	-0.12	-0.31	-0.38	-0.35	-0.20	0.04	0.04	-0.01	0.20	-0.07	0.04	0.02	0.02	0.04	0.14	0.00
9	HR 7899	-0.09	0.37	-0.13	-0.31	-0.41	-0.33	-0.20	0.04	0.06	-0.02	0.26	-0.03	0.06	0.01	0.04	0.06	0.13	0.00
10	38 OPH	-0.04	0.51	-0.10	-0.26	-0.37	-0.26	-0.20	0.08	0.05	0.00	0.25	-0.09	0.05	0.00	0.01	0.04	0.14	0.01
11	HR 7174	0.01	0.74	-0.09	-0.24	-0.29	-0.26	-0.18	0.15	0.03	-0.01	0.28	-0.14	0.03	0.03	0.05	0.06	0.15	0.02
12	9 VUL	0.01	0.75	-0.08	-0.23	-0.30	-0.24	-0.15	0.10	0.04	-0.01	0.24	-0.11	0.03	0.04	0.04	0.05	0.15	0.01
13	HD 189689	0.04	0.86	-0.11	-0.21	-0.31	-0.18	-0.14	0.12	0.04	-0.02	0.21	-0.15	0.03	0.00	0.04	0.05	0.15	0.01
14	THETA VIR	0.02	1.27	-0.03	-0.20	-0.24	-0.19	-0.10	0.14	0.12	0.01	0.47	-0.15	0.03	0.02	0.03	0.05	0.16	0.01
15	NU CAP	0.02	1.13	-0.01	-0.20	-0.22	-0.21	-0.07	0.19	0.07	-0.01	0.38	-0.20	0.03	0.01	0.05	0.08	0.16	0.00
16	HR 6169	0.15	1.20	0.01	-0.23	-0.23	-0.23	-0.12	0.29	0.08	0.01	0.44	-0.22	0.02	0.04	0.05	0.11	0.14	0.00
17	HD 190849A	0.11	1.13	0.00	-0.20	-0.25	-0.19	-0.11	0.34	0.08	0.01	0.37	-0.29	0.03	0.00	0.04	0.10	0.17	0.02
18	69 HER	0.06	1.22	0.02	-0.21	-0.20	-0.26	-0.07	0.27	0.13	0.00	0.42	-0.19	0.02	0.03	0.05	0.12	0.15	0.00
19	HD 190849B	0.15	1.16	0.04	-0.16	-0.23	-0.17	-0.10	0.35	0.08	0.00	0.32	-0.18	0.04	-0.01	0.05	0.18	0.17	0.01
20	58 AQL	0.16	1.25	0.02	-0.12	-0.20	-0.11	-0.12	0.13	0.12	-0.01	0.46	-0.17	0.05	0.01	0.04	0.07	0.13	0.03
21	78 HER	0.17	1.22	0.03	-0.17	-0.20	-0.15	-0.12	0.24	0.11	0.01	0.47	-0.19	0.04	0.00	0.03	0.08	0.14	0.01
22	HR 6570	0.23	1.14	0.13	-0.14	-0.19	-0.17	-0.13	0.31	0.11	0.03	0.38	-0.08	0.05	0.00	0.05	0.12	0.14	0.01
23	HD 187754	0.25	1.37	0.04	-0.10	-0.14	-0.10	-0.05	0.37	0.06	0.02	0.30	-0.25	0.02	0.00	0.05	0.10	0.17	0.02
24	THETA1 SER	0.13	1.16	0.13	-0.11	-0.11	-0.16	-0.09	0.28	0.14	-0.01	0.39	0.00	0.04	0.00	0.04	0.16	0.16	0.03
25	PRAE 276	0.25	1.23	0.11	-0.09	-0.13	-0.12	-0.05	0.41	0.06	0.03	0.25	-0.28	0.02	-0.02	0.06	0.18	0.14	0.01
26	PRAE 114	0.21	1.13	0.13	-0.07	-0.09	-0.12	-0.02	0.36	0.07	0.05	0.31	-0.04	0.03	-0.01	0.07	0.06	0.17	0.02
27	PRAE 154	0.22	1.05	0.14	-0.03	-0.09	-0.10	-0.01	0.37	0.05	0.03	0.24	-0.04	0.03	0.01	0.07	0.11	0.18	0.01
28	HD 190192	0.29	1.05	0.14	-0.02	-0.05	-0.07	-0.07	0.37	0.04	0.02	0.23	-0.01	0.02	-0.02	0.06	0.12	0.17	-0.01
29	PRAE 226	0.26	0.95	0.17	0.02	-0.02	-0.07	-0.03	0.37	0.05	0.03	0.22	0.05	0.00	-0.01	0.09	0.12	0.19	0.01
30	PRAE 37	0.28	0.88	0.20	0.05	0.01	-0.07	-0.02	0.35	0.08	0.05	0.26	0.15	0.00	0.00	0.09	0.09	0.19	0.01
31	HD 191177	0.36	0.92	0.24	0.04	0.08	-0.10	-0.06	0.22	0.16	0.04	0.09	0.15	0.02	0.05	0.08	0.11	0.16	0.01
32	PRAE 332	0.31	0.73	0.24	0.11	0.08	-0.04	0.01	0.33	0.10	-0.01	0.29	0.29	0.02	0.00	0.11	0.20	0.17	0.00
33	BD+293891	0.32	0.73	0.27	0.12	0.15	-0.06	-0.03	0.32	0.14	0.03	0.12	0.31	0.01	0.03	0.10	0.12	0.18	0.00
34	PRAE 222	0.28	0.68	0.28	0.15	0.10	0.01	-0.01	0.36	0.13	0.01	0.27	0.31	0.02	-0.04	0.12	0.16	0.20	-0.02
35	HD 35296	0.34	0.61	0.34	0.19	0.20	0.03	0.02	0.37	0.11	0.01	0.31	0.37	0.00	-0.01	0.12	0.19	0.20	0.05
36	BD+263780	0.36	0.63	0.32	0.20	0.23	-0.03	0.01	0.39	0.13	-0.05	-0.07	0.20	0.01	0.04	0.12	0.22	0.18	-0.01
37	HD 148816	0.46	0.56	0.20	0.25	0.17	0.11	-0.02	0.36	0.07	-0.05	0.25	0.41	0.00	-0.05	0.16	0.31	0.18	0.00
38	HD 155675	0.34	0.59	0.32	0.21	0.20	0.10	-0.08	0.31	0.10	-0.04	0.26	0.29	0.01	-0.04	0.13	0.25	0.22	0.06
39	PRAE 418	0.38	0.62	0.34	0.22	0.19	0.01	0.03	0.40	0.23	0.01	0.29	0.40	0.01	-0.01	0.15	0.22	0.20	0.00
40	HYAD 1	0.37	0.68	0.36	0.21	0.22	0.01	0.02	0.44	0.17	-0.01	0.29	0.41	0.00	0.00	0.17	0.23	0.22	0.00
41	HD 122693	0.39	0.72	0.33	0.20	0.24	-0.01	-0.02	0.44	0.16	-0.01	0.29	0.44	-0.08	0.00	0.17	0.29	0.21	0.02
42	HD 154417	0.36	0.61	0.34	0.23	0.20	0.02	-0.02	0.42	0.17	-0.03	0.30	0.49	0.05	-0.04	0.13	0.27	0.19	-0.03
43	HYAD 2	0.39	0.65	0.39	0.25	0.22	0.05	0.01	0.47	0.23	-0.05	0.28	0.43	0.04	-0.05	0.19	0.30	0.23	0.03
44	HD 227547	0.43	0.63	0.41	0.26	0.26	0.05	-0.03	0.44	0.23	-0.04	0.37	0.48	0.01	0.00	0.17	0.29	0.23	0.04
45	HD 154760	0.41	0.61	0.40	0.26	0.24	0.09	-0.07	0.44	0.18	-0.03	0.27	0.33	0.00	-0.05	0.17	0.26	0.24	0.05

© American Astronomical Society • Provided by the NASA Astrophysics Data System

1983ApJS...52..121G

TABLE 2—*Continued*

ID	NAME	SCAN "CONTINUUM" COLORS							FEATURE INDICES							ST			
		33-37	37-40	40-46	46-V	V-70	70-87	87-99	BREAK	CN38+	41-42	CA H	CA K	TI61+	TI71+	CA42	CH43	MG51	NA D
46	HD 190605	0.44	0.70	0.40	0.25	0.25	0.01	0.02	0.54	0.21	-0.06	-0.08	0.35	-0.01	0.02	0.16	0.26	0.20	0.01
47	HYAD 15	0.44	0.65	0.42	0.28	0.23	0.09	0.01	0.50	0.32	-0.02	0.25	0.36	0.00	-0.04	0.17	0.27	0.24	0.03
48	HD 139777A	0.49	0.57	0.46	0.28	0.31	0.02	0.02	0.47	0.12	0.00	0.07	0.14	0.00	0.00	0.20	0.26	0.20	0.00
49	HD 136274	0.49	0.73	0.47	0.30	0.33	0.08	0.01	0.57	0.49	-0.05	0.23	0.50	-0.05	-0.02	0.24	0.39	0.30	0.03
50	HYAD 26	0.45	0.68	0.50	0.33	0.30	0.09	0.03	0.58	0.47	-0.03	0.24	0.36	0.00	-0.03	0.22	0.35	0.29	0.05
51	HD 150205	0.61	0.69	0.43	0.35	0.28	0.12	0.02	0.56	0.34	-0.04	0.25	0.53	-0.01	-0.02	0.21	0.35	0.21	0.02
52	HYAD 21	0.47	0.71	0.58	0.35	0.31	0.14	0.04	0.66	0.56	-0.06	0.20	0.43	0.00	-0.03	0.27	0.45	0.31	0.00
53	+02 3001	0.51	0.70	0.60	0.38	0.43	0.10	0.06	0.63	0.28	0.02	-0.04	0.16	0.00	-0.01	0.28	0.28	0.23	0.02
54	HD 190571	0.65	0.73	0.60	0.42	0.40	0.18	-0.01	0.58	0.55	0.02	0.34	0.48	0.00	-0.02	0.21	0.35	0.26	0.04
55	HYAD 183	0.56	0.79	0.74	0.44	0.41	0.21	0.06	0.74	0.61	0.01	0.14	0.33	0.00	-0.03	0.31	0.34	0.38	0.04
56	HD 190470	0.63	0.80	0.73	0.45	0.43	0.18	0.03	0.79	0.61	0.01	0.05	0.36	0.00	-0.03	0.35	0.41	0.40	0.13
57	HD 154712	0.53	0.95	0.90	0.47	0.55	0.21	0.07	0.85	0.45	-0.01	-0.10	0.26	-0.02	-0.01	0.41	0.38	0.37	0.05
58	HYAD 185	0.56	0.90	0.95	0.56	0.59	0.33	0.11	0.82	0.53	-0.07	0.05	0.27	0.03	-0.04	0.45	0.40	0.43	-0.01
59	+38 2457	0.56	1.09	1.01	0.52	0.64	0.22	0.06	1.02	0.39	-0.06	-0.15	0.34	-0.06	-0.02	0.49	0.41	0.45	0.12
60	HYAD 173	0.67	1.03	1.18	0.64	0.67	0.41	0.13	0.94	0.38	-0.10	0.01	0.15	0.03	-0.02	0.58	0.44	0.47	0.18
61	GL 40	0.70	1.09	1.21	0.71	0.77	0.49	0.14	0.88	0.23	-0.07	-0.17	0.09	0.01	-0.06	0.53	0.36	0.42	0.13
62	HYAD 189	0.68	1.06	1.31	0.74	0.79	0.49	0.16	0.88	0.33	-0.15	-0.10	0.12	0.07	0.01	0.64	0.44	0.47	-0.01
63	HD 151288	0.79	1.10	1.23	0.78	0.79	0.50	0.13	0.93	0.24	-0.11	-0.21	0.17	0.05	0.01	0.59	0.38	0.40	0.17
64	HD 157881	0.77	1.05	1.28	0.76	0.81	0.56	0.07	0.84	0.32	-0.14	0.05	0.14	0.08	-0.01	0.63	0.44	0.49	0.29
65	HD 132683	0.66	1.17	1.25	0.77	0.86	0.52	0.12	0.88	0.28	-0.13	-0.27	0.11	0.08	0.02	0.63	0.40	0.43	0.26
66	GL 15A	0.93	1.11	1.19	0.98	1.02	0.91	0.22	0.74	0.26	-0.16	-0.16	0.10	0.20	0.07	0.61	0.42	0.34	0.16
67	GL 49	0.91	1.11	1.17	0.93	1.03	0.90	0.24	0.85	0.12	-0.13	-0.33	-0.17	0.21	0.10	0.00	0.35	0.34	0.00
68	GL 109	1.07	1.17	1.12	0.99	1.18	1.16	0.30	0.81	0.16	-0.23	-0.25	-0.01	0.34	0.22	0.61	0.41	0.35	0.23
69	GL 15B	1.15	1.28	1.34	1.15	1.31	1.45	0.33	0.57	0.43	-0.23	-0.17	0.25	0.46	0.24	0.78	0.48	0.38	0.20
70	GL 83.1	0.17	1.59	1.40	1.18	1.50	1.64	0.41	0.72	0.11	-0.14	-0.90	-0.06	0.43	0.37	0.78	0.48	0.38	0.35
71	GL 65	0.14	1.02	1.62	1.28	1.73	2.12	0.61	1.10	-0.86	-0.14	-1.75	-1.68	0.54	0.50	0.76	0.58	0.51	0.33
72	HR 7567	-0.11	0.17	-0.18	-0.33	-0.44	-0.42	-0.23	0.04	-0.02	-0.04	0.12	0.02	0.05	0.06	0.04	0.05	0.13	0.00
73	HR 7591	-0.13	0.19	-0.17	-0.34	-0.40	-0.39	-0.23	0.01	0.01	-0.03	0.15	0.01	0.03	0.04	0.04	0.06	0.15	0.00
74	20 AQL	-0.05	0.48	-0.12	-0.26	-0.36	-0.29	-0.22	0.04	0.03	-0.01	0.22	-0.04	0.03	0.02	0.01	0.03	0.13	0.00
75	HR 7467	-0.08	0.47	-0.13	-0.29	-0.38	-0.32	-0.23	0.08	0.02	-0.01	0.19	-0.10	0.04	0.02	0.02	0.03	0.16	0.00
76	IOTA LYR	0.01	0.60	-0.10	-0.25	-0.33	-0.27	-0.14	0.08	0.03	0.00	0.17	-0.11	0.04	0.03	0.03	0.05	0.16	0.00
77	HR 7346	-0.02	0.76	-0.09	-0.25	-0.31	-0.28	-0.17	0.15	0.03	-0.02	0.25	-0.14	0.02	0.04	0.03	0.04	0.15	0.00
78	59 HER	0.16	1.24	0.00	-0.25	-0.30	-0.19	-0.10	0.29	0.06	0.01	0.31	-0.22	0.03	-0.02	0.04	0.09	0.16	0.01
79	HR 6642	0.11	1.09	-0.01	-0.22	-0.30	-0.21	-0.14	0.19	0.10	0.00	0.44	-0.17	0.03	0.01	0.04	0.09	0.15	0.03
80	11 SGE	0.06	1.10	-0.03	-0.20	-0.24	-0.22	-0.15	0.16	0.10	0.00	0.36	-0.19	0.02	0.04	0.03	0.07	0.14	0.00
81	60 HER	0.12	1.17	0.12	-0.16	-0.15	-0.21	-0.07	0.29	0.13	0.03	0.36	-0.13	0.03	0.02	0.05	0.13	0.15	0.00
82	HD 192285	0.22	1.16	0.08	-0.11	-0.16	-0.12	-0.08	0.37	0.07	0.02	0.32	-0.13	0.05	0.01	0.05	0.10	0.17	0.01
83	ALPHA OPH	0.16	1.20	0.12	-0.10	-0.11	-0.15	-0.07	0.30	0.10	0.00	0.32	-0.08	0.01	0.01	0.08	0.25	0.16	0.01
84	HD 165475B	0.25	1.16	0.17	-0.03	-0.08	-0.12	-0.08	0.41	0.06	0.06	0.26	-0.13	0.01	0.01	0.08	0.08	0.13	0.01
85	HD 165475	0.31	1.15	0.10	0.02	0.05	-0.05	-0.07	0.32	0.06	0.02	0.20	-0.16	0.00	0.05	0.05	0.10	0.15	0.00
86	XI SER	0.19	1.08	0.22	-0.03	-0.02	-0.11	-0.05	0.25	0.12	0.05	0.29	0.07	0.03	0.01	0.08	0.15	0.16	0.04
87	HD 5132	0.23	0.97	0.19	0.03	0.00	-0.11	-0.01	0.33	0.08	0.06	0.23	-0.04	0.02	-0.01	0.08	0.09	0.16	0.01
88	HD 508	0.32	1.07	0.18	0.04	0.00	-0.06	0.01	0.33	0.10	0.01	0.32	0.16	0.01	-0.01	0.09	0.14	0.16	0.01
89	HD 210875	0.32	1.05	0.22	0.04	-0.01	-0.07	-0.02	0.39	0.07	0.05	0.24	-0.01	0.02	-0.02	0.08	0.12	0.17	0.02
90	RHO CAP	0.23	0.83	0.24	0.07	0.09	-0.05	-0.04	0.28	0.09	0.02	0.25	0.23	0.04	-0.02	0.09	0.13	0.15	0.00

TABLE 2—*Continued*

ID	NAME	SCAN "CONTINUUM" COLORS							FEATURE INDICES							ST			
		33-37	37-40	40-46	46-V	V-70	70-87	87-99	BREAK	CN38+	41-42	CA H	CA K	TI61+	TI71+	CA42	CH43	MG51	NA D
91	HD 7331	0.33	0.72	0.28	0.13	0.10	-0.03	0.01	0.38	0.12	-0.02	0.28	0.29	0.02	-0.02	0.11	0.21	0.19	0.00
92	BD+630013	0.32	0.65	0.30	0.15	0.08	0.00	-0.01	0.38	0.16	0.00	0.29	0.38	0.02	-0.04	0.13	0.19	0.20	0.00
93	HD 13391	0.37	0.68	0.36	0.23	0.19	0.05	0.01	0.41	0.22	-0.04	0.13	0.32	0.00	-0.03	0.17	0.27	0.16	0.02
94	HD 154962	0.47	0.68	0.45	0.29	0.28	0.06	0.00	0.50	0.50	-0.01	0.30	0.53	-0.01	0.00	0.17	0.37	0.22	0.00
95	HD 192344	0.47	0.69	0.46	0.29	0.25	0.09	0.00	0.51	0.48	-0.01	0.31	0.42	0.01	-0.03	0.18	0.33	0.25	0.01
96	HR 6516	0.46	0.66	0.51	0.27	0.24	0.09	-0.06	0.50	0.47	-0.04	0.31	0.58	0.00	-0.01	0.22	0.37	0.24	0.04
97	HR 7670	0.52	0.71	0.53	0.29	0.25	0.08	-0.02	0.56	0.54	0.01	0.27	0.49	0.01	-0.02	0.20	0.38	0.24	0.01
98	HD 128428	0.57	0.72	0.51	0.35	0.31	0.07	0.02	0.51	0.63	0.04	0.27	0.55	0.02	0.00	0.20	0.38	0.22	0.03
99	31 AQL	0.52	0.73	0.50	0.35	0.35	-0.01	-0.03	0.48	0.66	0.01	0.22	0.55	-0.01	0.01	0.25	0.42	0.25	0.03
100	-02 4018	0.58	0.72	0.65	0.37	0.43	0.08	0.04	0.67	0.38	0.03	-0.02	0.21	0.02	-0.02	0.28	0.29	0.28	0.01
101	M67 F143?	0.54	0.82	0.58	0.42	0.41	0.10	0.04	0.62	0.48	0.05	0.11	0.46	-0.04	-0.01	0.32	0.34	0.24	0.05
102	HD 11004	0.57	0.87	0.52	0.47	0.42	0.24	0.10	0.48	0.26	0.05	0.10	0.25	-0.03	-0.04	0.17	0.24	0.16	0.01
103	HD 173399A	0.63	0.76	0.61	0.41	0.38	0.20	0.03	0.59	0.51	0.03	0.29	0.48	-0.01	-0.03	0.22	0.34	0.24	-0.03
104	HD 56176	0.61	0.75	0.64	0.44	0.43	0.19	0.10	0.63	0.51	0.02	0.35	0.50	-0.01	0.00	0.28	0.43	0.26	0.02
105	HD 227693	0.68	0.81	0.67	0.47	0.42	0.20	0.01	0.57	0.54	0.12	0.39	0.58	0.01	-0.02	0.20	0.30	0.24	0.06
106	HD 199580	0.70	0.89	0.70	0.45	0.47	0.14	0.05	0.74	0.58	0.07	-0.17	0.37	0.01	0.03	0.24	0.32	0.22	-0.01
107	HD 152306	0.68	0.81	0.69	0.48	0.46	0.10	0.02	0.59	0.38	0.03	0.00	0.21	-0.01	0.03	0.18	0.37	0.17	0.00
108	PRAE 212	0.71	0.85	0.70	0.47	0.38	0.21	0.05	0.63	0.75	0.18	0.32	0.50	0.01	-0.04	0.23	0.32	0.22	0.03
109	THETA1 TAU	0.76	0.83	0.72	0.48	0.40	0.21	0.09	0.63	0.76	0.21	0.35	0.57	0.02	-0.01	0.22	0.38	0.25	0.03
110	HD 170527	0.72	0.81	0.75	0.49	0.45	0.21	0.05	0.63	0.50	0.07	0.24	0.46	0.01	0.00	0.20	0.34	0.19	0.00
111	HD 136366	0.83	0.87	0.77	0.50	0.44	0.25	0.02	0.61	0.75	0.22	0.40	0.71	-0.01	-0.01	0.23	0.35	0.20	0.05
112	HD 191615	0.76	0.93	0.73	0.51	0.49	0.20	0.09	0.72	0.54	0.08	0.05	0.37	-0.01	0.00	0.25	0.35	0.22	0.01
113	HD 124679	0.70	0.85	0.77	0.50	0.43	0.21	0.04	0.66	0.72	0.19	0.33	0.61	0.01	-0.02	0.23	0.36	0.23	0.01
114	HD 131111	0.70	0.88	0.79	0.51	0.49	0.26	0.06	0.68	0.74	0.10	0.41	0.75	-0.01	-0.01	0.29	0.44	0.24	-0.01
115	HD 113439	0.79	1.00	0.77	0.51	0.52	0.14	0.04	0.78	0.72	0.11	0.25	0.62	-0.06	0.00	0.30	0.42	0.25	0.04
116	HD 4744	0.78	0.93	0.76	0.55	0.51	0.28	0.11	0.72	0.42	0.03	0.11	0.41	-0.04	-0.04	0.27	0.36	0.20	0.02
117	HD 7010	0.75	0.90	0.76	0.55	0.48	0.26	0.11	0.71	0.54	0.09	0.07	0.40	-0.01	-0.03	0.29	0.35	0.21	0.03
118	46 L MI	0.78	0.88	0.84	0.54	0.50	0.26	0.07	0.72	0.79	0.18	0.33	0.64	0.02	-0.02	0.27	0.39	0.27	-0.01
119	91 AQR	0.80	0.95	0.89	0.54	0.47	0.23	0.08	0.75	0.82	0.19	0.35	0.69	-0.05	-0.05	0.30	0.42	0.27	0.03
120	M67 F141	0.77	1.04	0.83	0.54	0.50	0.19	0.07	0.82	0.79	0.21	0.23	0.63	-0.05	-0.05	0.30	0.38	0.27	0.05
122	HD 140301	0.85	0.96	0.91	0.55	0.49	0.29	0.04	0.15	0.03	-0.02	0.25	-0.14	0.02	0.04	0.03	0.04	0.15	0.00
123	HD 95272	0.81	0.92	0.88	0.57	0.49	0.29	0.09	0.29	0.06	0.01	0.31	-0.22	0.03	-0.02	0.04	0.09	0.16	0.01
124	HD 72184	0.87	0.96	0.93	0.56	0.48	0.26	0.10	0.19	0.10	0.00	0.44	-0.17	0.03	0.01	0.04	0.09	0.15	0.03
125	HD 119425	0.72	0.97	0.93	0.56	0.49	0.25	0.05	0.16	0.10	0.00	0.36	-0.19	0.02	0.04	0.03	0.07	0.14	0.00
126	HD 106760	0.78	0.96	0.94	0.59	0.55	0.26	0.06	0.29	0.13	0.03	0.36	-0.13	0.03	0.02	0.05	0.13	0.15	0.00
127	PSI U MA	0.87	0.94	0.98	0.60	0.55	0.28	0.08	0.37	0.07	0.02	0.32	-0.13	0.05	0.01	0.05	0.10	0.17	0.01
128	PHI SER	0.89	1.03	0.98	0.57	0.46	0.27	0.03	0.30	0.10	0.00	0.32	-0.08	0.01	0.01	0.08	0.25	0.16	0.01
129	HD 136514	0.96	1.06	1.08	0.60	0.52	0.32	0.04	0.41	0.06	0.06	0.26	-0.13	0.01	0.01	0.08	0.08	0.13	0.01
130	MU AQL	0.82	1.09	1.05	0.61	0.57	0.24	0.07	0.32	0.06	0.02	0.20	-0.16	0.00	0.05	0.05	0.10	0.15	0.00
131	HR 5227	0.95	1.04	0.99	0.65	0.57	0.28	-0.01	0.25	0.12	0.05	0.29	0.07	0.03	0.01	0.08	0.15	0.16	0.04
132	HD 154759	0.94	1.07	1.11	0.65	0.65	0.22	0.12	0.33	0.08	0.06	0.23	-0.04	0.02	-0.01	0.08	0.09	0.16	0.01
133	20 CYG	1.03	1.17	1.21	0.67	0.55	0.31	0.06	0.33	0.10	0.01	0.32	0.16	0.01	-0.01	0.09	0.14	0.16	0.01
134	ALPH SER	0.85	1.03	1.01	0.60	0.51	0.30	0.07	0.39	0.07	0.05	0.24	-0.01	0.02	-0.02	0.08	0.12	0.17	0.02
135	MU LEO	0.95	1.08	1.11	0.66	0.57	0.31	0.09	0.28	0.09	0.02	0.25	0.23	0.04	-0.02	0.09	0.13	0.15	0.00

© American Astronomical Society • Provided by the NASA Astrophysics Data System

© American Astronomical Society • Provided by the NASA Astrophysics Data System

1983ApJS...52..121G

TABLE 2—*Continued*

ID	NAME	SCAN "CONTINUUM" COLORS							FEATURE INDICES							ST			
		33-37	37-40	40-46	46-V	V-70	70-87	87-99	BREAK	CN38+	41-42	CA H	CA K	TI61+	TI71+	CA42	CH43	MG51	NA D
136	+1 3131	0.79	1.10	0.89	0.70	0.62	0.25	0.07	0.86	0.48	0.13	-0.10	0.19	-0.01	-0.01	0.30	0.40	0.23	0.01
137	M67 F170	1.03	1.21	1.18	0.72	0.67	0.30	0.12	1.02	0.76	0.29	0.20	0.63	-0.04	-0.01	0.40	0.37	0.33	0.08
138	18 LIB A	0.86	1.18	1.14	0.67	0.57	0.36	0.07	0.77	0.98	0.35	0.28	0.84	0.05	-0.02	0.44	0.44	0.32	0.07
139	+28 2165	1.00	1.20	1.19	0.74	0.71	0.32	0.09	1.10	0.50	0.21	0.10	0.60	-0.04	0.00	0.42	0.38	0.34	0.05
140	NGC 188-1	0.90	1.10	1.12	0.73	0.64	0.36	0.15	0.83	0.96	0.27	0.41	0.76	0.01	-0.02	0.39	0.39	0.29	0.08
141	+30 2344	1.02	1.29	1.21	0.74	0.73	0.32	0.12	1.07	0.57	0.17	0.28	0.62	-0.03	-0.01	0.42	0.39	0.33	0.04
142	HD 83618	0.90	1.10	1.20	0.75	0.67	0.38	0.12	0.97	0.67	0.25	0.33	0.72	0.01	-0.02	0.38	0.39	0.33	0.05
143	HD 158885	1.02	1.03	1.13	0.76	0.67	0.42	0.06	0.87	0.83	0.29	0.33	0.52	0.01	-0.06	0.35	0.42	0.37	0.10
144	HD 166780	1.09	1.21	1.33	0.78	0.73	0.42	0.06	1.02	0.61	0.20	0.37	0.64	0.05	-0.01	0.48	0.44	0.37	0.11
145	HD 148513	1.02	1.26	1.45	0.83	0.65	0.47	0.10	1.01	0.69	0.32	0.39	0.74	0.08	0.03	0.50	0.40	0.38	0.12
146	M67 T626	1.03	1.22	1.38	0.85	0.74	0.42	0.16	1.06	0.62	0.27	0.34	0.70	0.06	0.00	0.00	0.00	0.00	0.06
147	HD 127227	1.06	1.40	1.44	0.83	0.84	0.44	0.13	1.10	0.54	0.23	0.12	0.53	0.11	0.09	0.55	0.41	0.39	0.14
148	M67 IV-202	1.11	1.34	1.53	0.90	0.89	0.45	0.17	1.06	0.50	0.20	0.27	0.63	0.13	0.11	0.55	0.42	0.41	0.11
149	HD 50778	1.06	1.38	1.37	0.84	0.78	0.49	0.21	0.88	0.62	0.23	0.69	0.81	0.08	0.01	0.46	0.42	0.39	0.09
150	HD 62721	1.09	1.28	1.40	0.84	0.82	0.48	0.20	1.11	0.49	0.16	0.37	0.56	0.14	0.08	0.51	0.46	0.45	0.10
151	HD 116870	0.94	1.35	1.44	0.86	0.89	0.51	0.18	1.02	0.52	0.20	0.31	0.71	0.16	0.12	0.53	0.49	0.42	0.08
152	HD 60522	1.09	1.29	1.57	0.92	0.94	0.53	0.22	1.11	0.43	0.22	0.33	0.53	0.22	0.17	0.58	0.45	0.45	0.13
153	-1 3113	1.24	1.69	1.56	1.07	0.93	0.61	0.18	1.14	0.46	0.28	-0.16	0.23	0.07	0.02	0.50	0.38	0.32	0.07
154	+2 2884	1.26	1.44	1.42	0.90	0.98	0.55	0.17	1.14	0.40	0.18	0.19	0.63	0.21	0.22	0.53	0.38	0.41	0.12
155	-2 3873	1.13	1.46	1.54	1.02	1.22	0.76	0.24	1.08	0.32	0.12	0.11	0.49	0.38	0.37	0.57	0.35	0.45	0.17
156	HD 104216	0.93	1.30	1.50	1.01	1.21	0.76	0.24	1.00	0.33	0.17	0.46	0.59	0.49	0.45	0.52	0.32	0.46	0.10
157	HD 142804	1.36	1.41	1.75	1.16	1.20	0.87	0.25	0.95	0.41	0.24	0.21	0.65	0.42	0.35	0.60	0.38	0.44	0.14
158	HD 30959	1.02	1.41	1.63	1.22	1.46	0.97	0.35	1.02	0.29	0.15	0.27	0.56	0.53	0.47	0.53	0.32	0.47	0.16
159	HD 151658	1.07	1.45	1.72	1.26	1.51	1.06	0.34	1.05	0.29	0.21	0.27	0.55	0.49	0.44	0.53	0.31	0.41	0.14
160	-2 4025	1.28	1.49	1.31	1.20	1.58	1.11	0.37	1.17	0.14	0.05	-0.08	0.50	0.49	0.65	0.52	0.29	0.48	0.16
161	-01 3097	1.70	1.52	1.29	1.17	1.62	1.21	0.43	1.04	0.22	0.09	-0.05	0.17	0.29	0.56	0.48	0.00	0.41	0.16
162	TX DRA	1.65	1.50	1.02	1.20	1.72	1.18	0.44	0.96	0.27	0.04	0.31	0.67	0.77	0.90	0.41	0.18	0.58	0.11
163	Z CYG	2.10	1.56	0.89	1.31	1.77	1.29	0.35	0.92	0.16	0.14	0.24	0.60	0.71	0.71	0.13	0.00	0.52	0.13
164	+01 3133	2.02	1.52	0.75	1.21	1.84	1.48	0.54	1.01	0.21	0.01	-0.03	0.19	0.37	0.74	0.35	0.10	0.42	0.18
165	-2 3886	1.75	1.54	0.56	1.33	2.03	1.54	0.54	1.05	0.17	-0.08	0.07	0.47	0.59	1.00	0.31	0.12	0.58	0.15
166	W HER	2.87	1.56	-0.86	1.40	2.53	2.01	0.63	0.96	0.24	-0.46	0.47	0.81	0.85	1.21	0.35	0.15	0.65	0.29
167	TY DRA	2.37	1.64	-0.21	1.61	2.41	1.86	0.92	1.01	0.34	-0.31	0.37	0.78	0.71	1.07	0.41	0.04	0.65	0.11
168	SW VIR	2.72	1.73	-0.64	1.88	2.73	2.09	1.01	0.84	0.41	-0.48	0.45	0.73	0.82	1.20	0.55	0.16	0.73	0.19
169	RZ HER	2.04	1.06	-0.99	1.78	2.97	2.34	1.24	0.33	0.27	-0.56	0.38	0.60	0.85	1.35	0.60	0.06	0.75	0.50
170	R LEO	0.11	1.69	-0.88	2.25	3.28	2.86	1.58	0.56	0.34	-0.36	0.32	0.34	0.87	1.11	0.73	-0.40	0.79	0.20
171	AW CYG	-2.88	0.94	4.24	4.46	1.66	1.24	0.13	0.01	1.56	0.37	0.40	-0.43	-0.22	0.19	0.82	0.77	-0.47	0.25
172	WZ CAS	-1.18	1.96	3.71	2.20	1.19	1.53	0.27	1.25	0.35	0.35	-0.02	0.30	0.23	-0.03	0.93	0.79	0.22	0.60
173	69 CYG	-0.15	-0.02	-0.18	-0.30	-0.45	-0.33	-0.25	-0.07	0.01	0.03	0.04	-0.02	0.04	0.04	0.03	0.04	0.15	-0.01
174	HR 7699	-0.01	0.45	-0.15	-0.29	-0.37	-0.35	-0.19	0.03	0.02	-0.01	0.14	0.02	0.03	0.05	0.02	0.05	0.13	0.00
175	HR 8020	0.18	0.27	-0.04	-0.09	-0.18	-0.16	-0.13	0.01	0.00	0.02	0.06	0.02	0.03	0.01	0.04	0.02	0.12	-0.02

1983ApJS...52..121G

TABLE 3

COLORS TRANSFORMED TO STANDARD SYSTEM

ID	$(U-B)_o$	$(B-V)_o$	$(R-I)_o$	ID	$(U-B)_o$	$(B-V)_o$	$(R-I)_o$	ID	$(U-B)_o$	$(B-V)_o$	$(R-I)_o$
DWARFS											
1	-1.23	-0.34		56	0.69	0.93	0.46	112	0.76	0.98	0.53
2	-1.20	-0.32		57	0.86	1.01	0.54	113	0.77	0.98	0.48
3	-1.17	-0.31		58	0.87	1.12	0.63	114	0.81	0.99	0.56
4	-1.04	-0.26		59	1.04	1.10	0.54	115	0.92	0.99	0.47
5	-1.00	-0.27		60	1.17	1.25	0.70	116	0.75	1.03	0.57
6	-0.92	-0.24		61	1.17	1.32	0.78	117	0.78	1.03	0.54
7	-0.78	-0.20		62		1.37	0.80	118	0.90	1.03	0.53
8	-0.76	-0.20		63		1.40	0.82	119	0.99	1.05	0.52
9	-0.74	-0.19		64		1.38	0.84	120	1.01	1.05	0.49
10	-0.59	-0.13		65		1.39	0.84	121	1.12	1.05	0.49
11	-0.39	-0.10						122	1.03	1.06	0.55
12	-0.38	-0.09						123	0.98	1.08	0.57
13	-0.33	-0.07						124	1.11	1.09	0.54
14	0.04	-0.02						125	1.03	1.08	0.52
15	-0.06	-0.01		GIANTS				126	1.06	1.12	0.55
16	0.07	-0.01		72	-0.95	-0.25		127	1.11	1.12	0.56
17	0.00	0.02		73	-0.93	-0.25		128	1.17	1.11	0.51
18	0.06	0.01		74	-0.64	-0.15		129	1.30	1.15	0.56
19	0.07	0.07		75	-0.66	-0.18		130	1.23	1.17	0.54
20	0.08	0.07		76	-0.51	-0.13		131	1.23	1.19	0.57
21	0.10	0.05		77	-0.39	-0.10		132	1.27	1.22	0.56
22	0.15	0.12		78	0.09	-0.04		133	1.55	1.24	0.57
23	0.23	0.14		79	-0.04	-0.03		134	1.22	1.14	0.57
24	0.11	0.16		80	-0.07	-0.02		135	1.38	1.22	0.58
25	0.20	0.17		81	0.12	0.10		136	1.07	1.19	0.59
26	0.14	0.19		82	0.13	0.14		137	1.52	1.28	0.62
27	0.10	0.23	0.11	83	0.13	0.17		138	1.38	1.23	0.64
28	0.10	0.25	0.12	84	0.20	0.24		139	1.50	1.31	0.65
29	0.07	0.29	0.16	85	0.14	0.26	0.19	140	1.40	1.28	0.68
30	0.04	0.32	0.16	86	0.14	0.26	0.13	141	1.55	1.31	0.66
31	0.11	0.33	0.17	87	0.07	0.30	0.13	142	1.41	1.31	0.68
32	-0.03	0.41	0.21	88	0.17	0.32	0.17	143	1.38	1.31	0.72
33	0.00	0.42	0.22	89	0.19	0.34	0.16	144	1.64	1.37	0.72
34	-0.02	0.45	0.26	90	0.03	0.36	0.20	145	1.79	1.44	0.73
35	-0.01	0.51	0.29	91	0.02	0.45	0.22	146	1.71	1.44	0.73
36	-0.02	0.53	0.29	92	-0.01	0.47	0.24	147	1.85	1.44	0.79
37	-0.14	0.53	0.33	93	0.07	0.57	0.28	148		1.52	0.83
38	-0.07	0.53	0.33	94	0.25	0.67	0.35	149		1.43	0.84
39	0.03	0.55	0.29	95	0.25	0.67	0.36	150		1.44	0.85
40	0.08	0.55	0.30	96	0.26	0.68	0.31	151		1.46	0.90
41	0.10	0.54	0.27	97	0.36	0.70	0.32	152		1.54	0.93
42	0.02	0.56	0.29	98	0.38	0.75	0.37	153		1.67	0.94
43	0.11	0.61	0.31	99	0.36	0.76	0.33	154		1.49	0.97
44	0.12	0.62	0.33	100	0.46	0.82	0.40				
45	0.09	0.61	0.34	101	0.50	0.84	0.41				
46	0.17	0.62	0.32	102	0.41	0.86	0.51				
47	0.17	0.65	0.35	103	0.49	0.84	0.47				
48	0.09	0.66	0.33	104	0.51	0.89	0.49				
49	0.29	0.70	0.37	105	0.62	0.90	0.47				
50	0.29	0.74	0.36	106	0.71	0.92	0.47				
51	0.27	0.73	0.39	107	0.57	0.92	0.42				
52	0.42	0.80	0.40	108	0.71	0.93	0.47				
53	0.35	0.82	0.43	109	0.75	0.94	0.48				
54	0.47	0.85	0.46	110	0.66	0.95	0.50				
55	0.65	0.92	0.48	111	0.80	0.97	0.51				

© American Astronomical Society • Provided by the NASA Astrophysics Data System

1983ApJS...52..121G

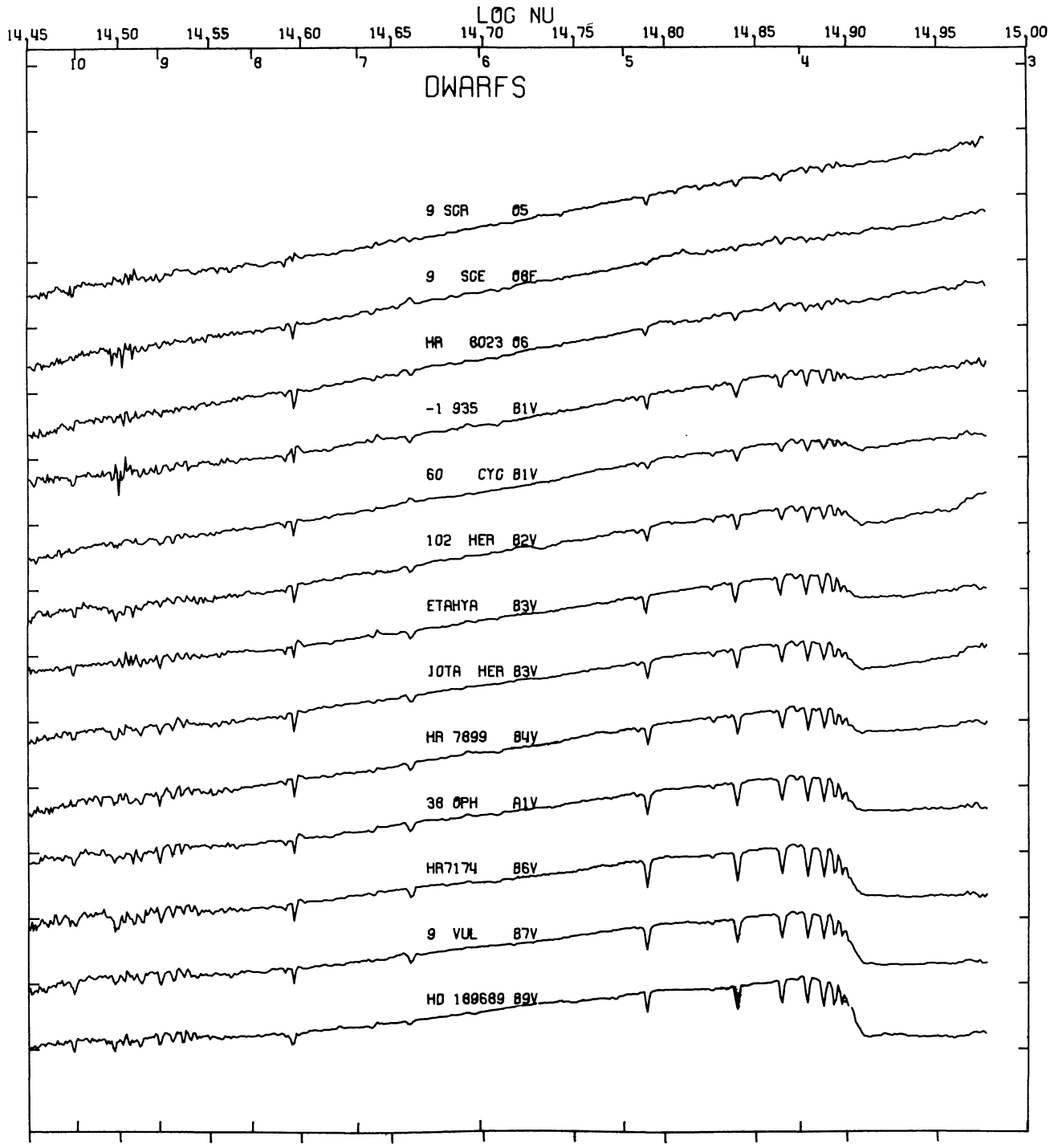

FIG. 2*a*.—Dwarfs O5–B9

FIG. 2*a–t*.—The Spectrophotometric Atlas. Scans are shown in order of $(B-V)_{\rm scan}$ for $B-V<1.10$ and in order of $(R-I)_{\rm scan}$ for $R-I>0.35$. The top abscissa has two scales: the upper is logarithmic in frequency; the lower is in 1000 A units. The ordinate tickmarks represent 1 mag each on an arbitrary scale.

© American Astronomical Society • Provided by the NASA Astrophysics Data System

1983ApJS...52..121G

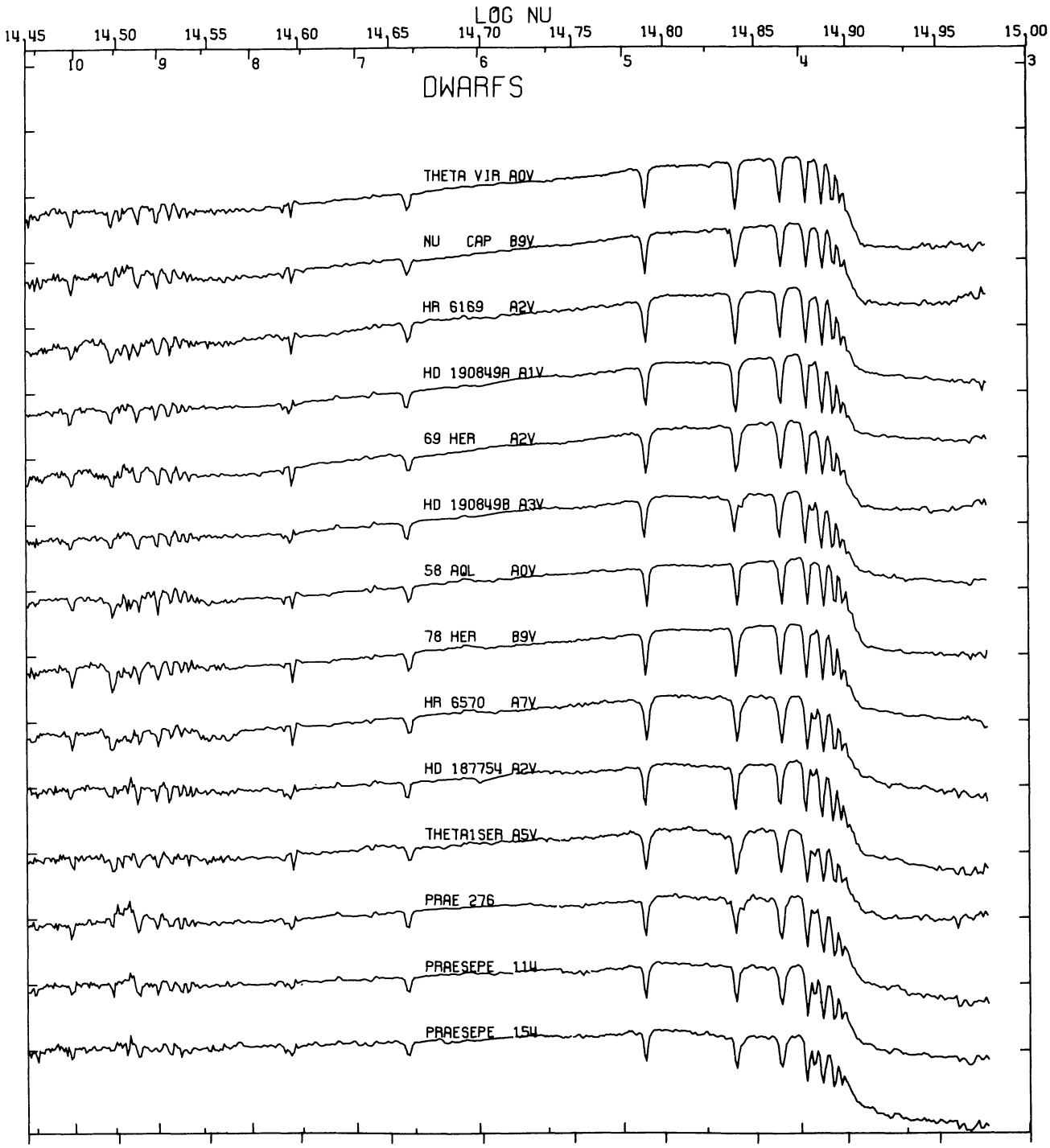

FIG. 2*b*.—Dwarfs A0–A5

© American Astronomical Society • Provided by the NASA Astrophysics Data System

1983ApJS...52..121G

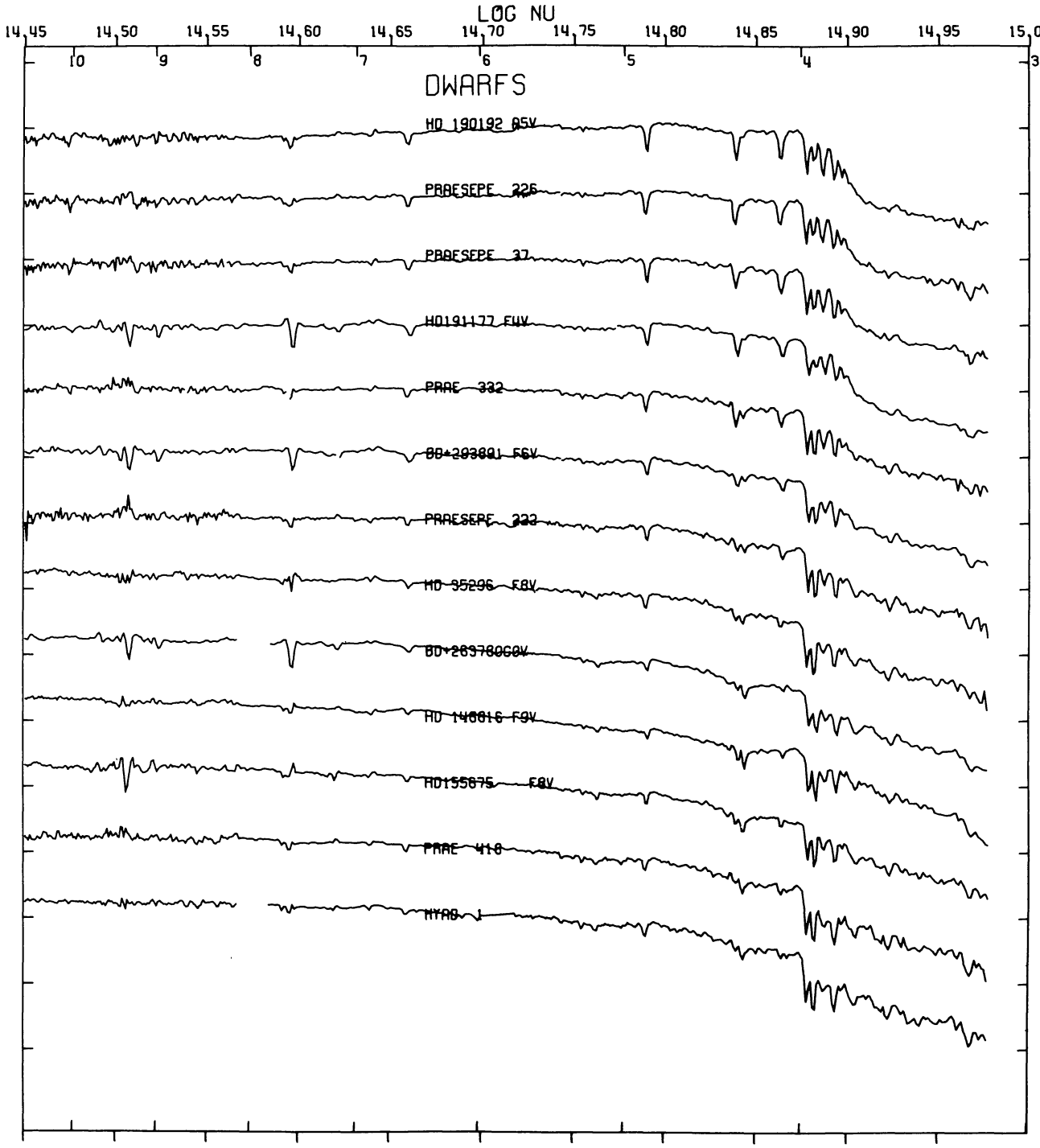

FIG. 2*c*.—Dwarfs A5–F8

© American Astronomical Society • Provided by the NASA Astrophysics Data System

1983ApJS...52..121G

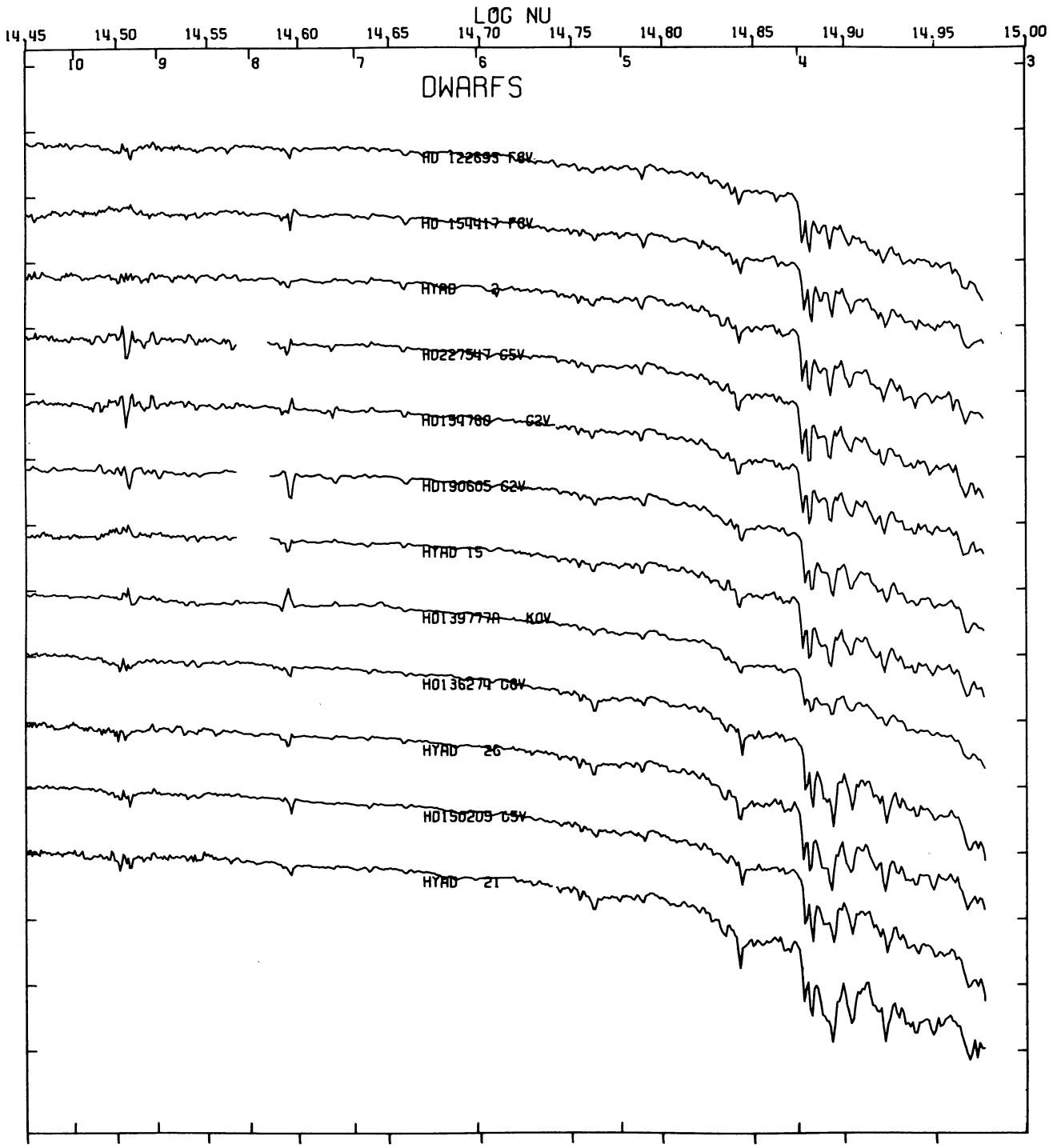

FIG. 2*d*.—Dwarfs F8–G5

© American Astronomical Society • Provided by the NASA Astrophysics Data System

1983ApJS...52..121G

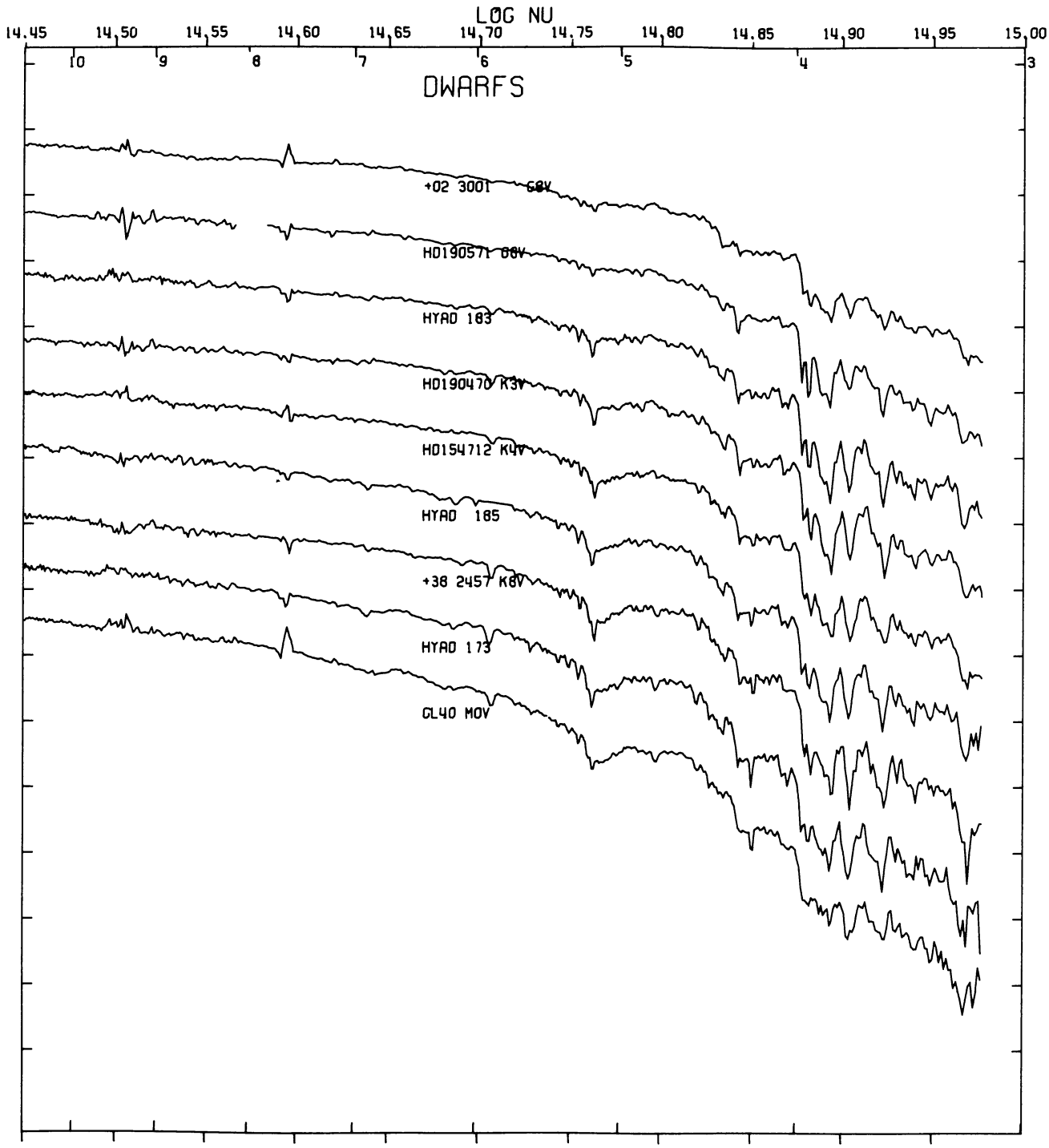

FIG. 2*e*.—Dwarfs G8–M0

© American Astronomical Society • Provided by the NASA Astrophysics Data System

1983ApJS...52..121G

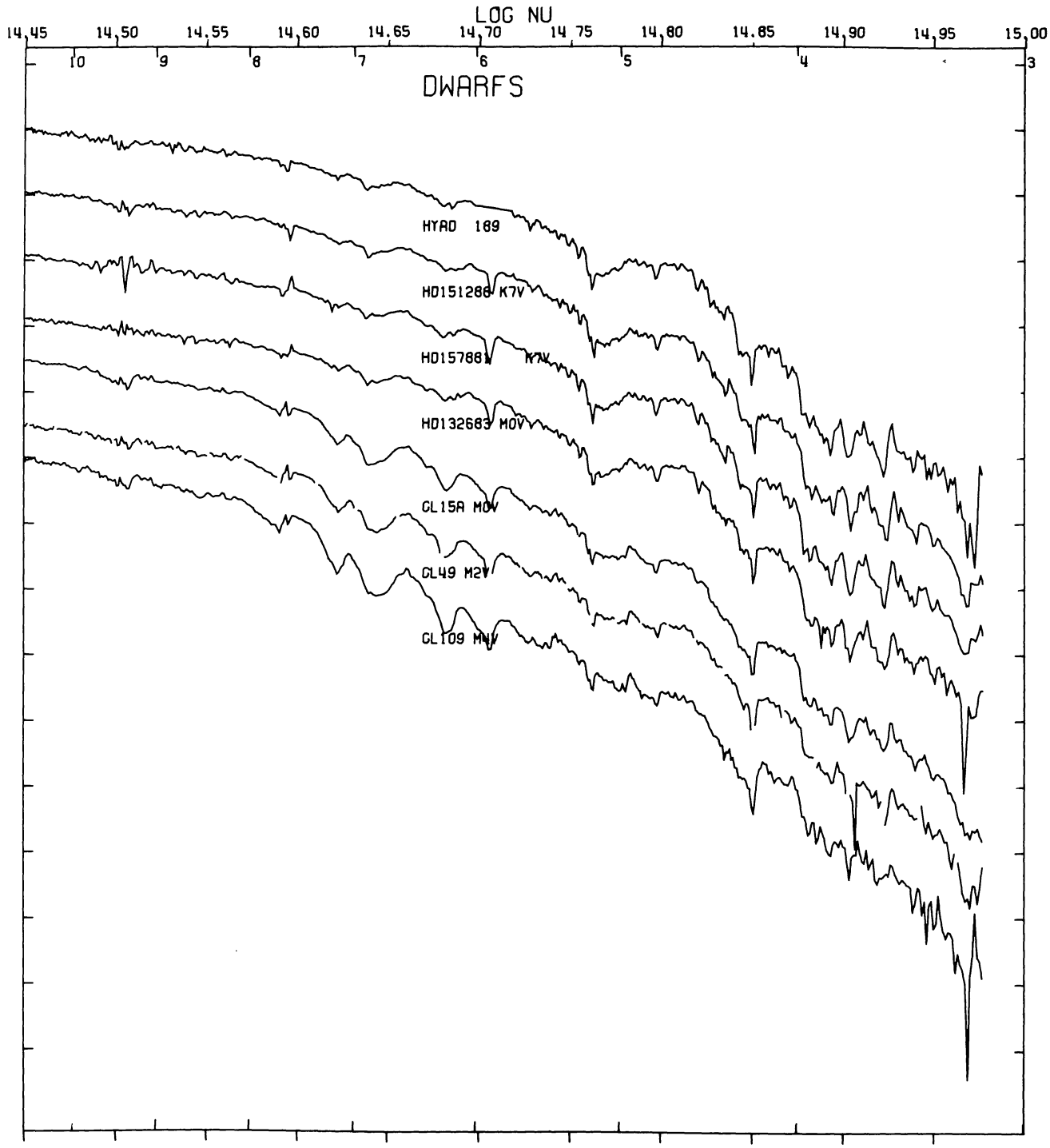

FIG. 2*f*.—Dwarfs K7–M4

© American Astronomical Society • Provided by the NASA Astrophysics Data System

1983ApJS...52..121G

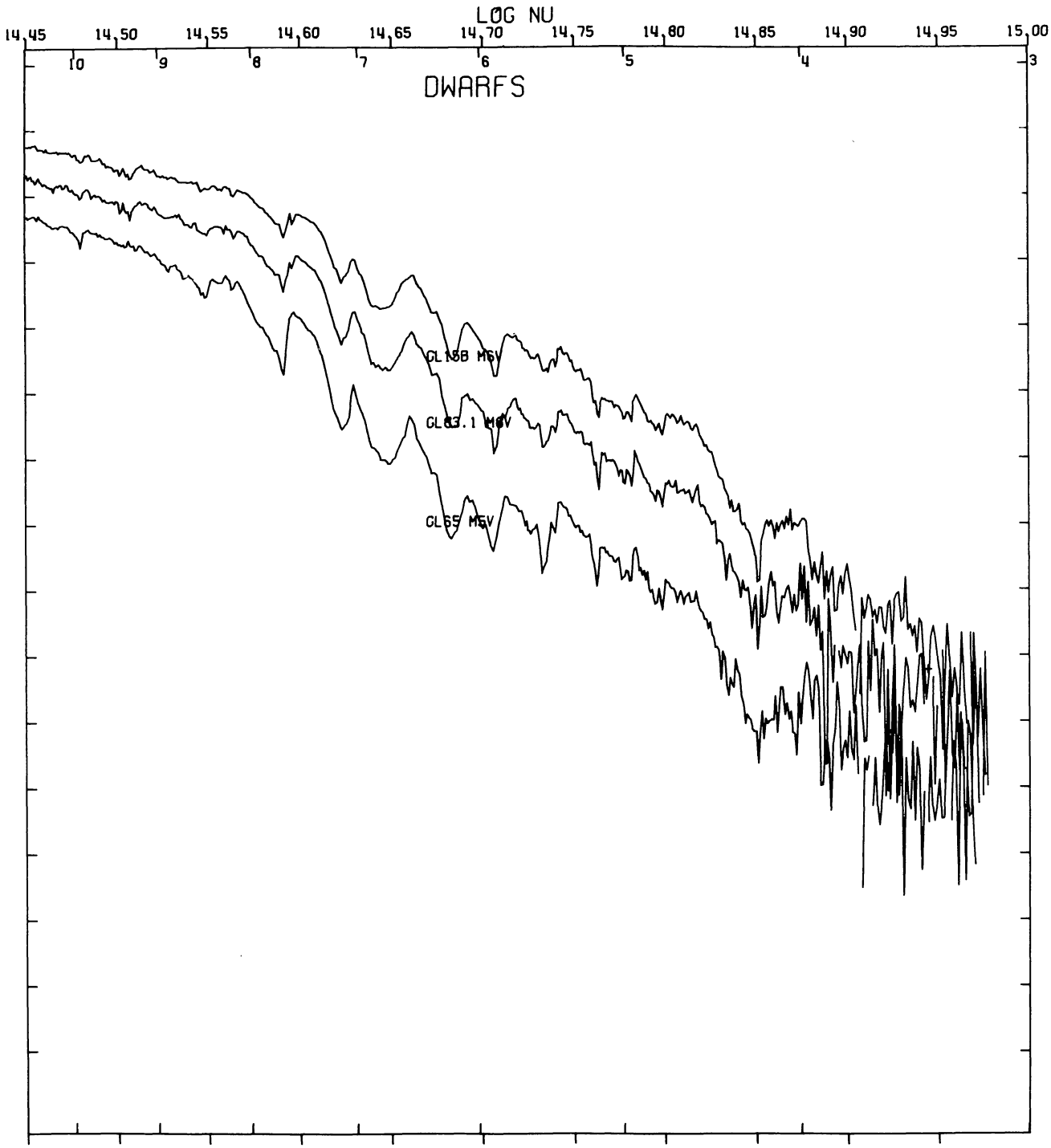

FIG. 2g.—Dwarfs M5–M8

© American Astronomical Society • Provided by the NASA Astrophysics Data System

1983ApJS...52..121G

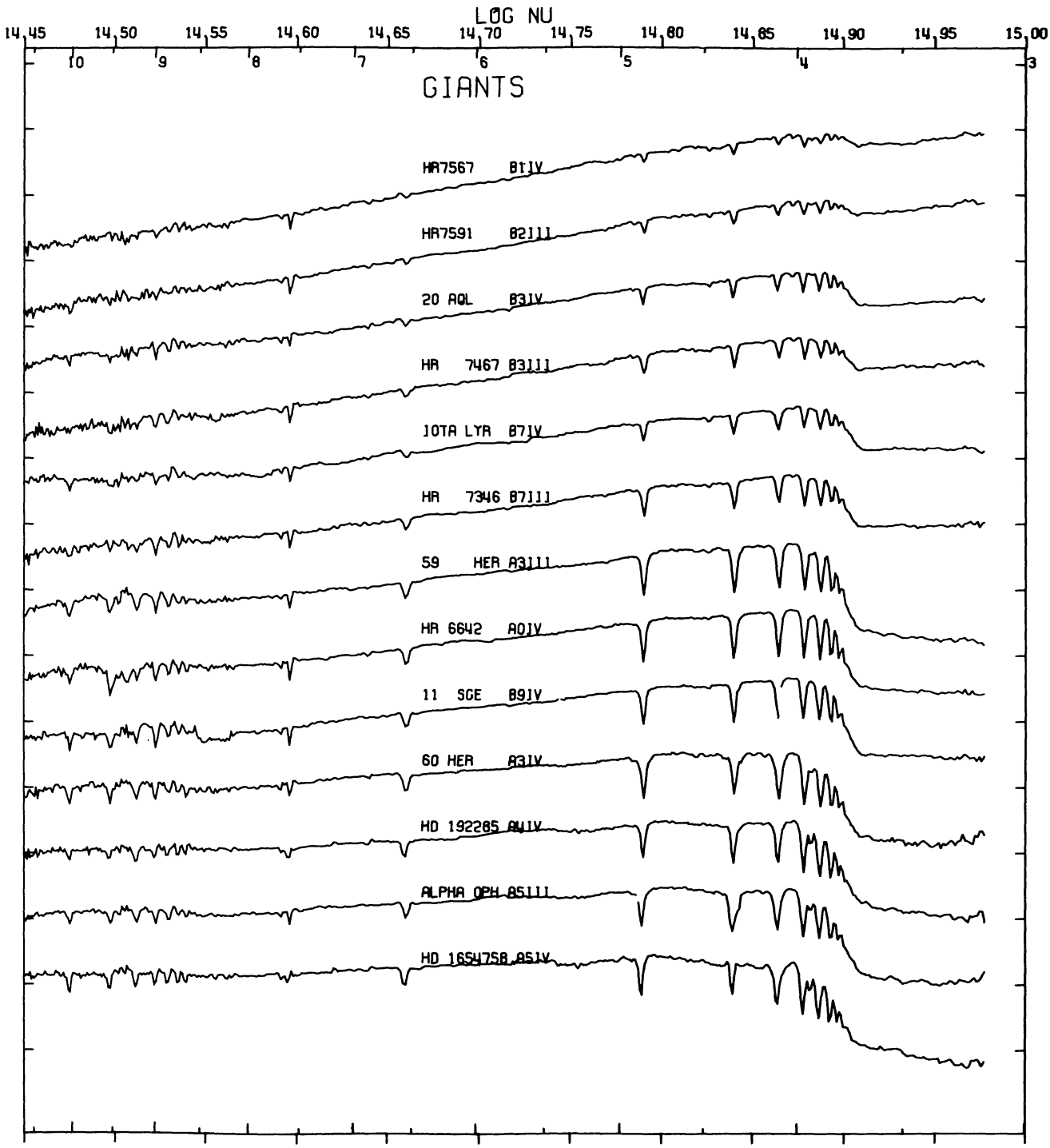

FIG. 2*h*.—Giants B1–A5

© American Astronomical Society • Provided by the NASA Astrophysics Data System

1983ApJS...52..121G

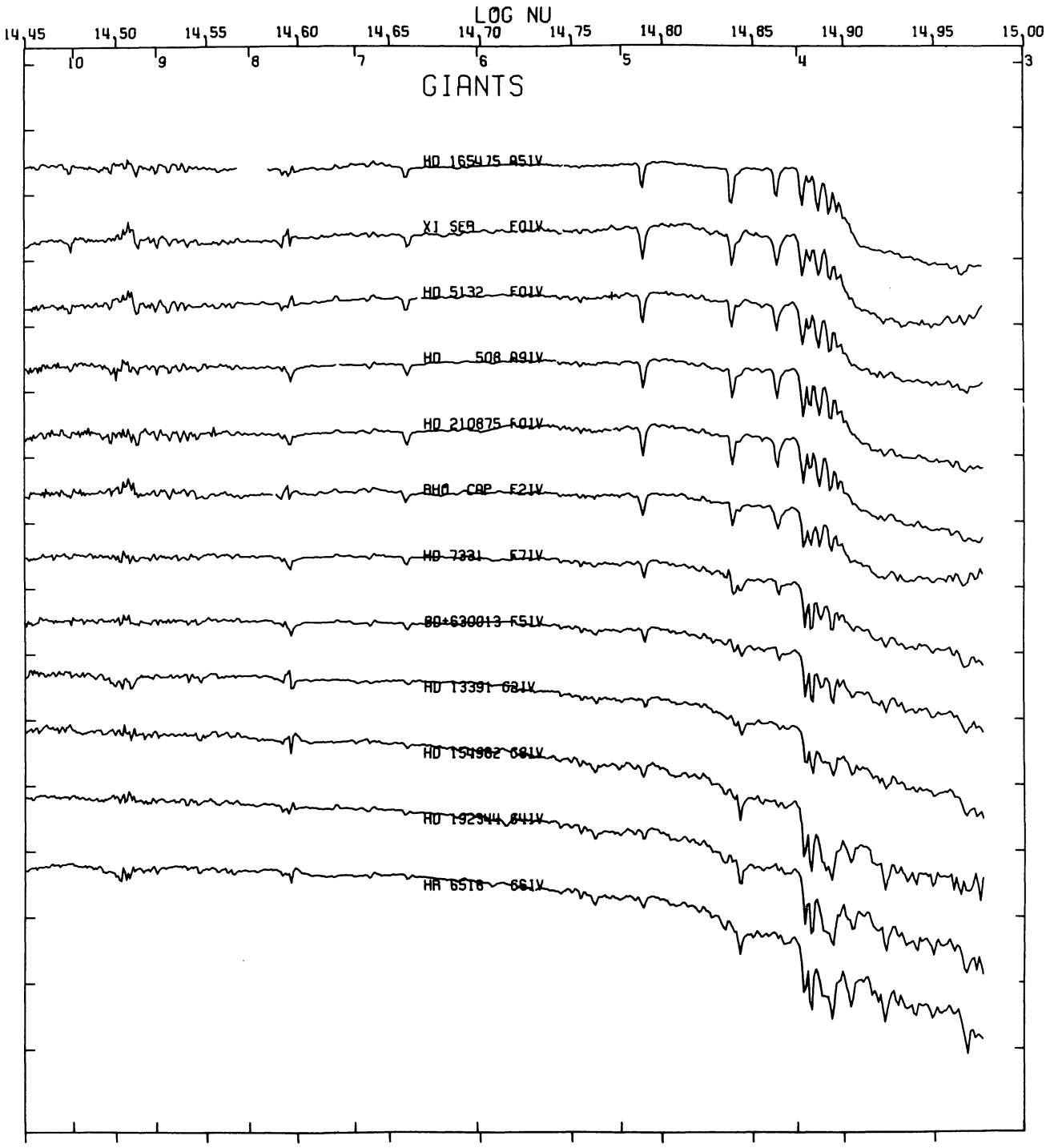

FIG. 2*i*.—Giants A5–G6

© American Astronomical Society • Provided by the NASA Astrophysics Data System

1983ApJS...52..121G

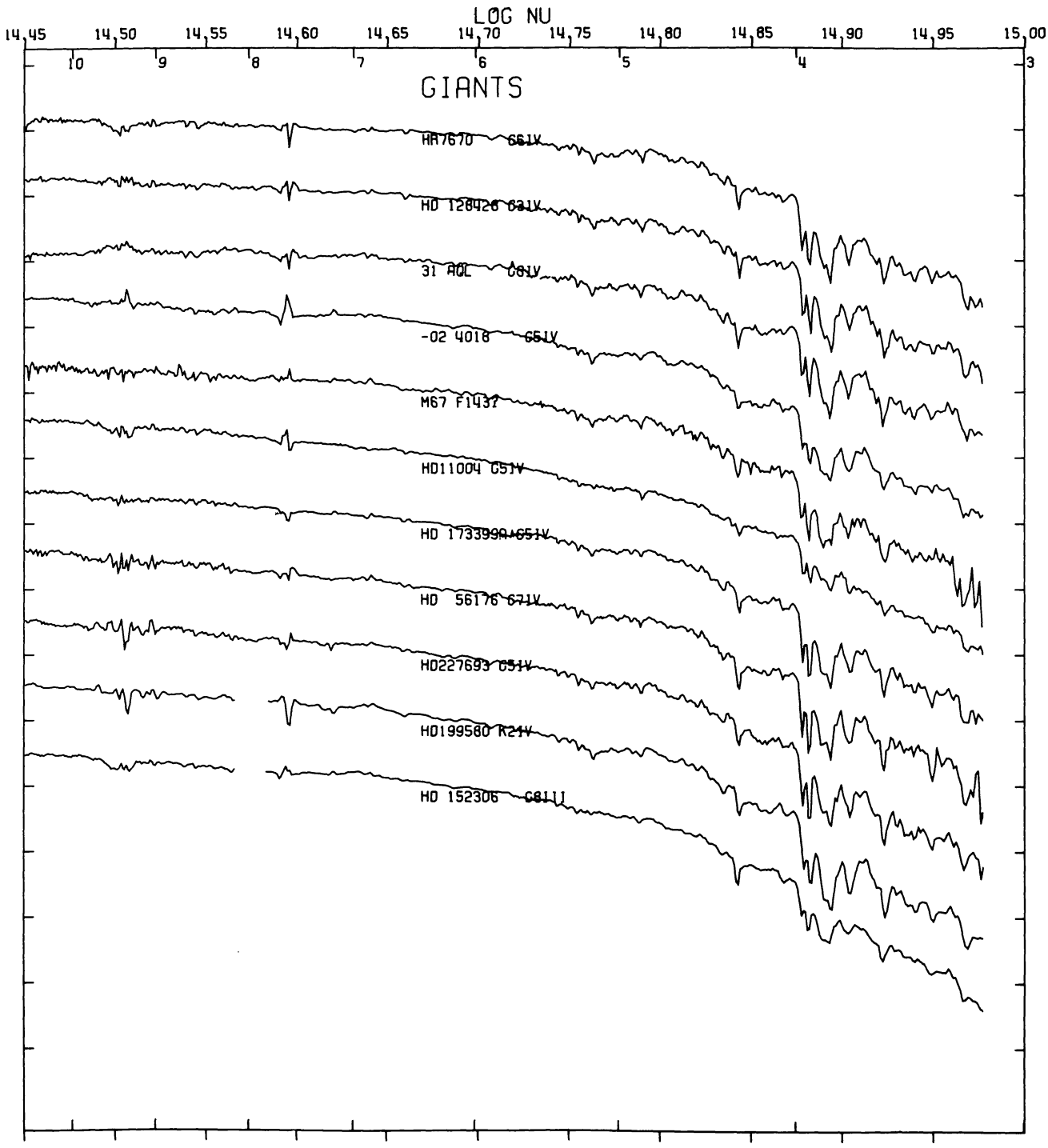

FIG. 2*j*.—Giants G6–G8

© American Astronomical Society • Provided by the NASA Astrophysics Data System

1983ApJS...52..121G

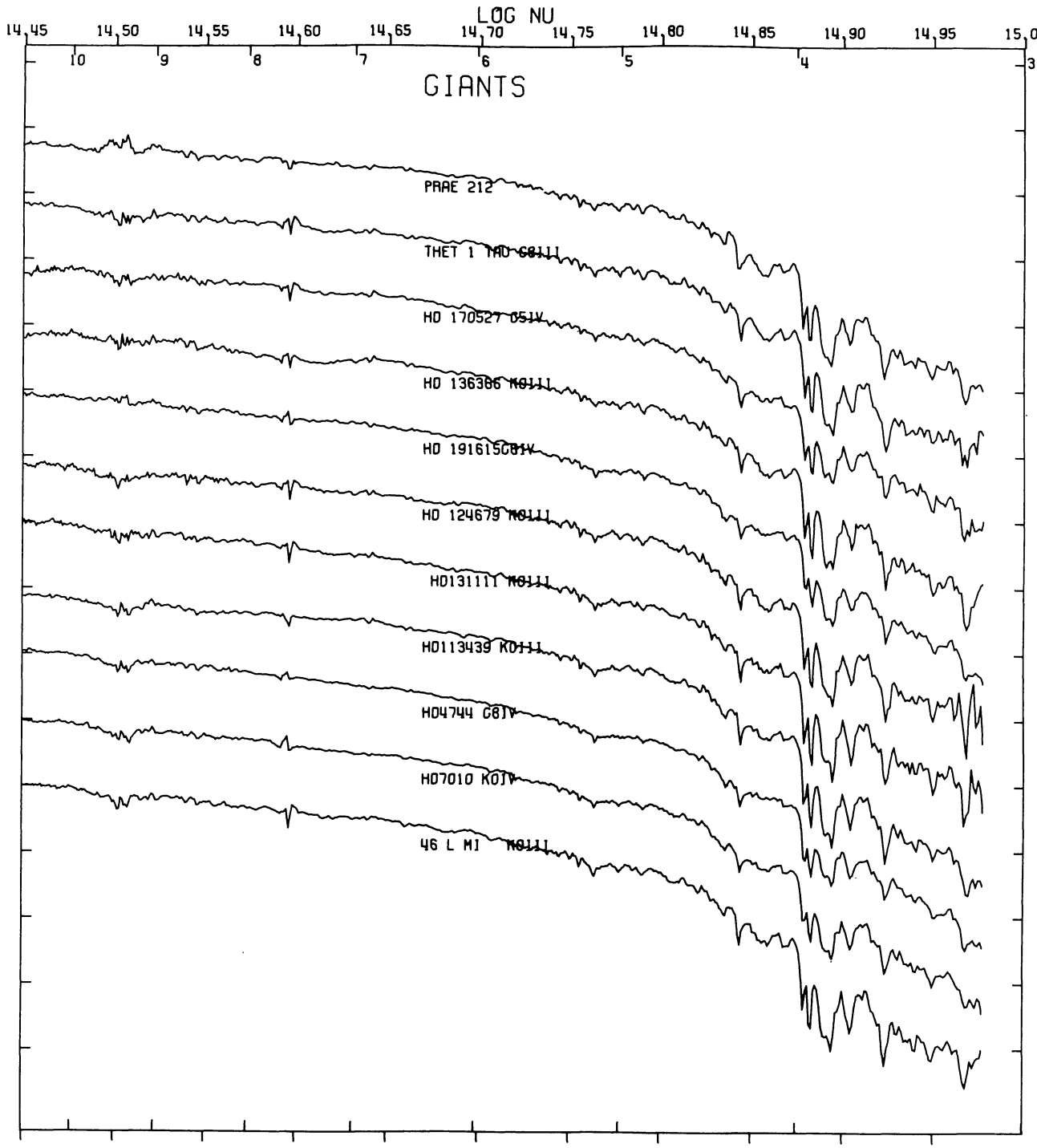

FIG. 2*k*.—Giants G8–K0

© American Astronomical Society • Provided by the NASA Astrophysics Data System

1983ApJS...52..121G

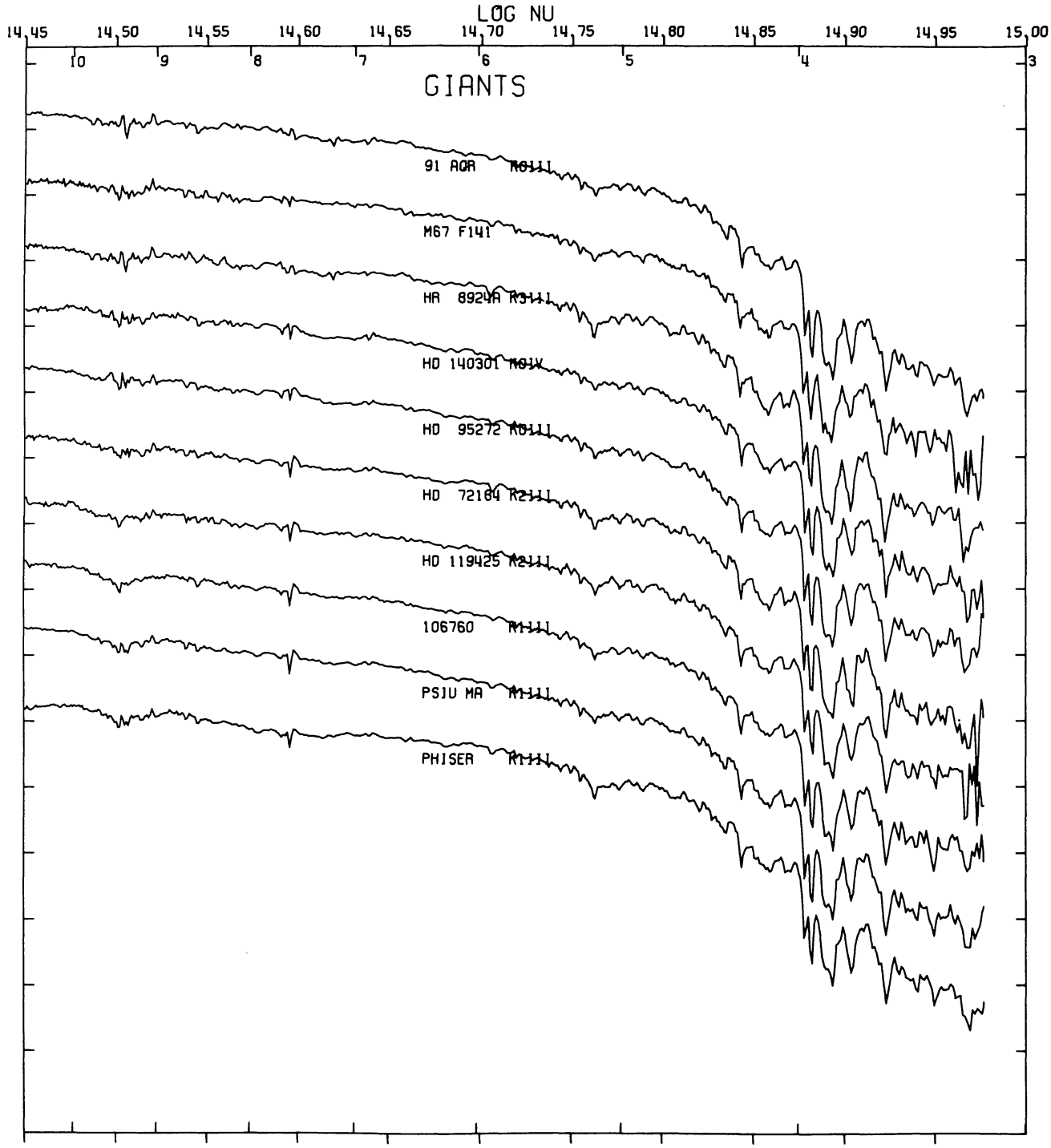

FIG. 2*l*.—Giants K0–K1

© American Astronomical Society • Provided by the NASA Astrophysics Data System

1983ApJS...52..121G

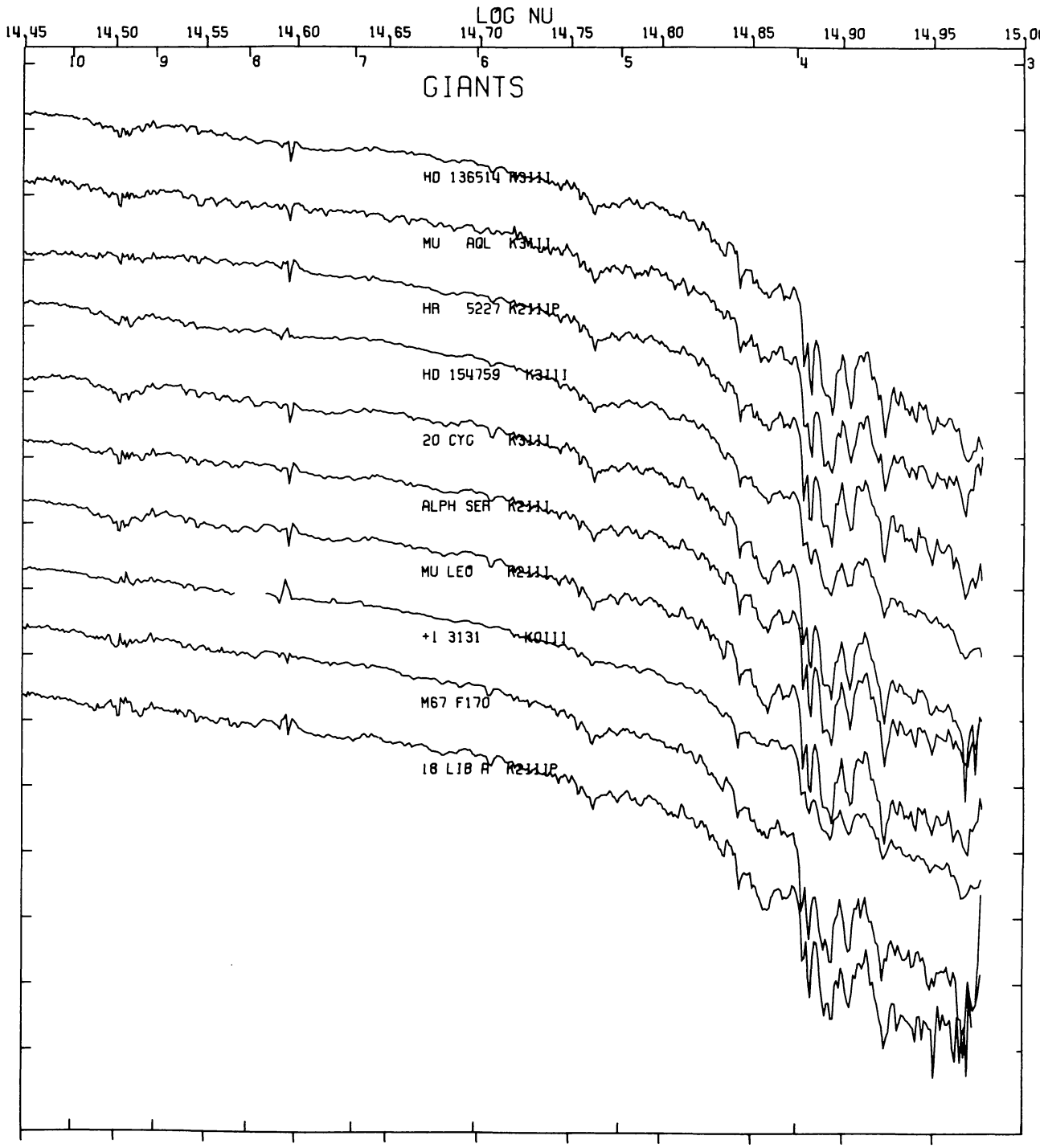

FIG. 2*m*.—Giants K2–K3

© American Astronomical Society • Provided by the NASA Astrophysics Data System

1983ApJS...52..121G

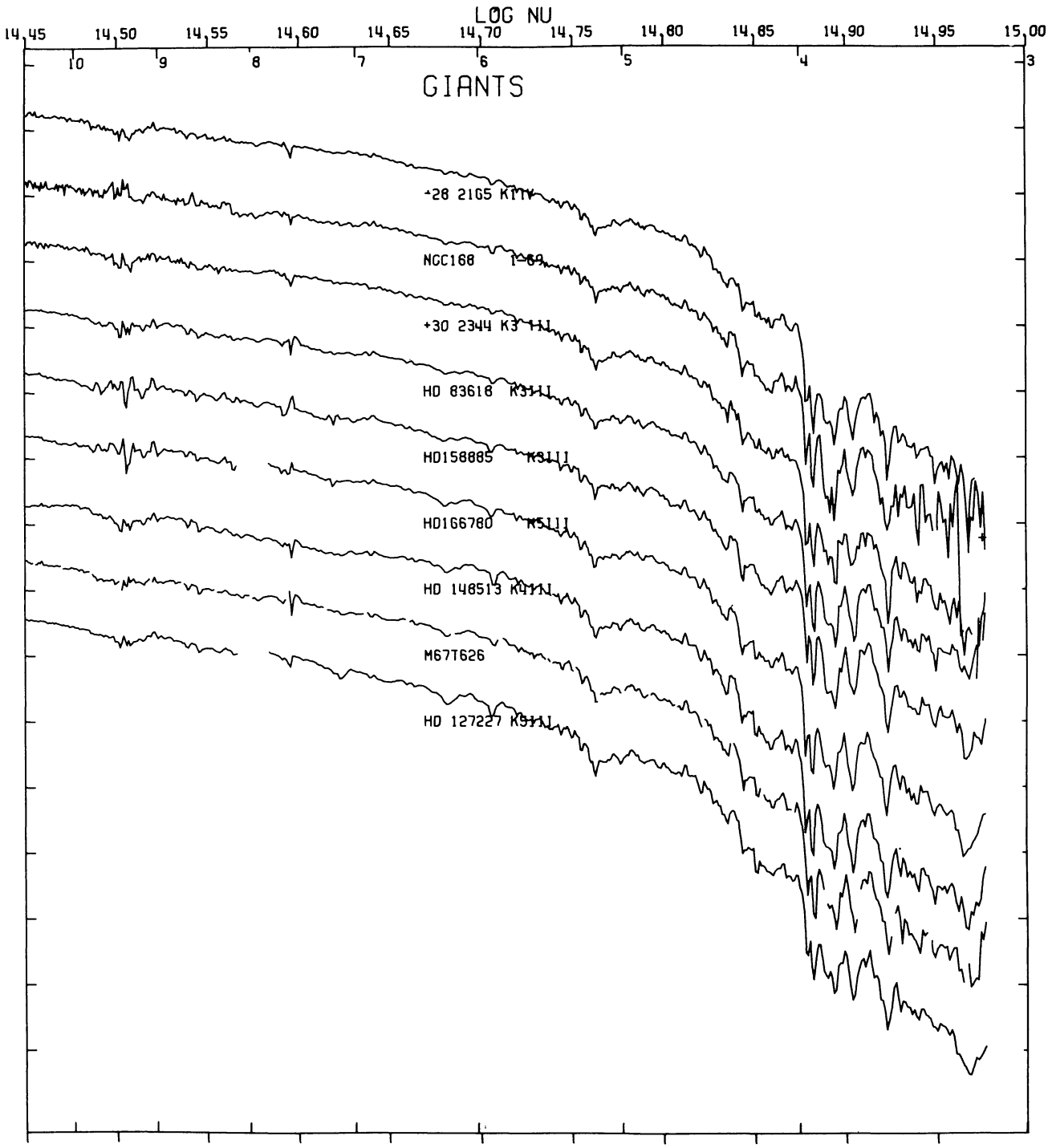

FIG. 2*n*.—Giants K1–K4

© American Astronomical Society • Provided by the NASA Astrophysics Data System

1983ApJS...52..121G

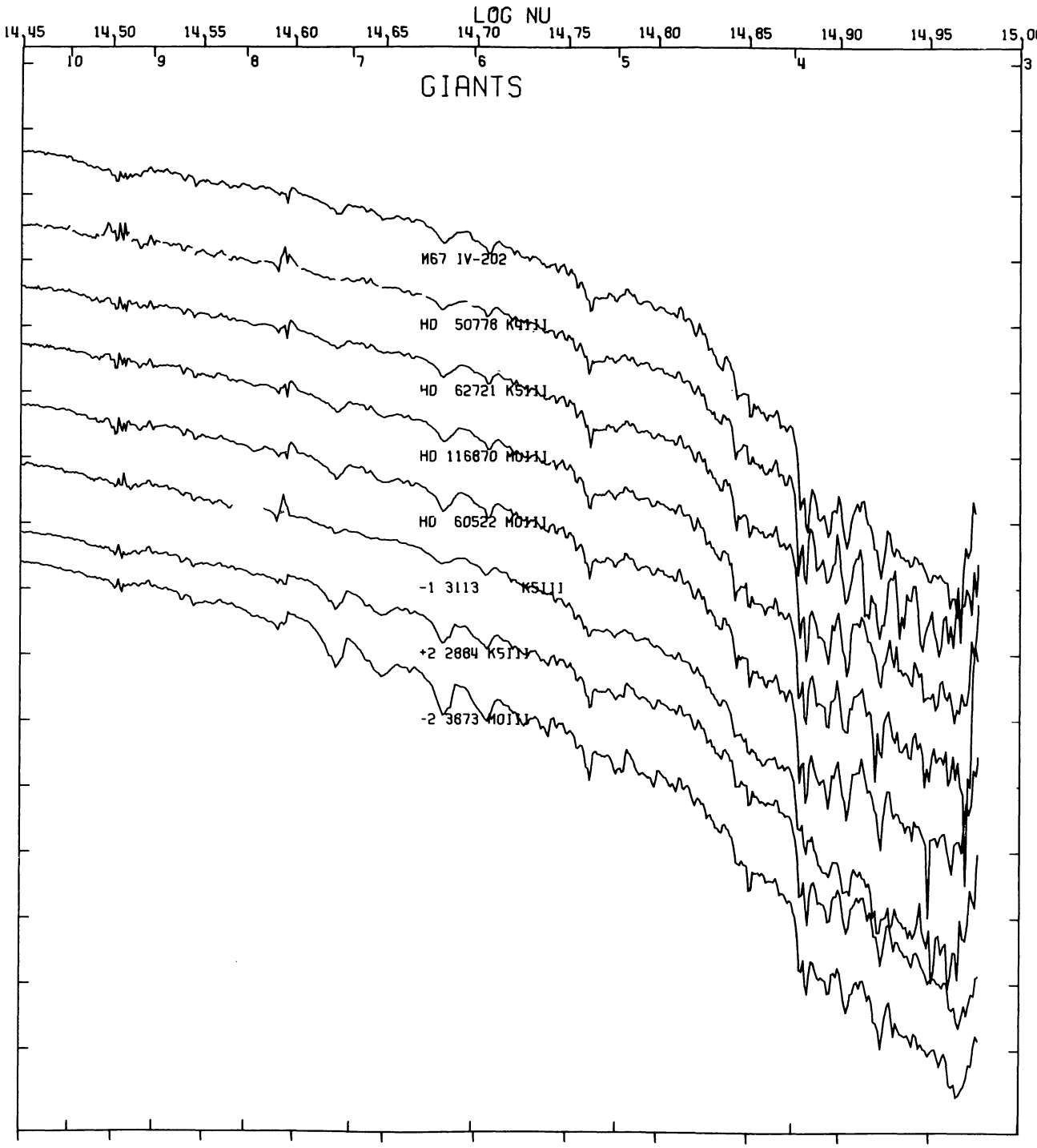

FIG. 2*o*.—Giants K4–M0

© American Astronomical Society • Provided by the NASA Astrophysics Data System

1983ApJS...52..121G

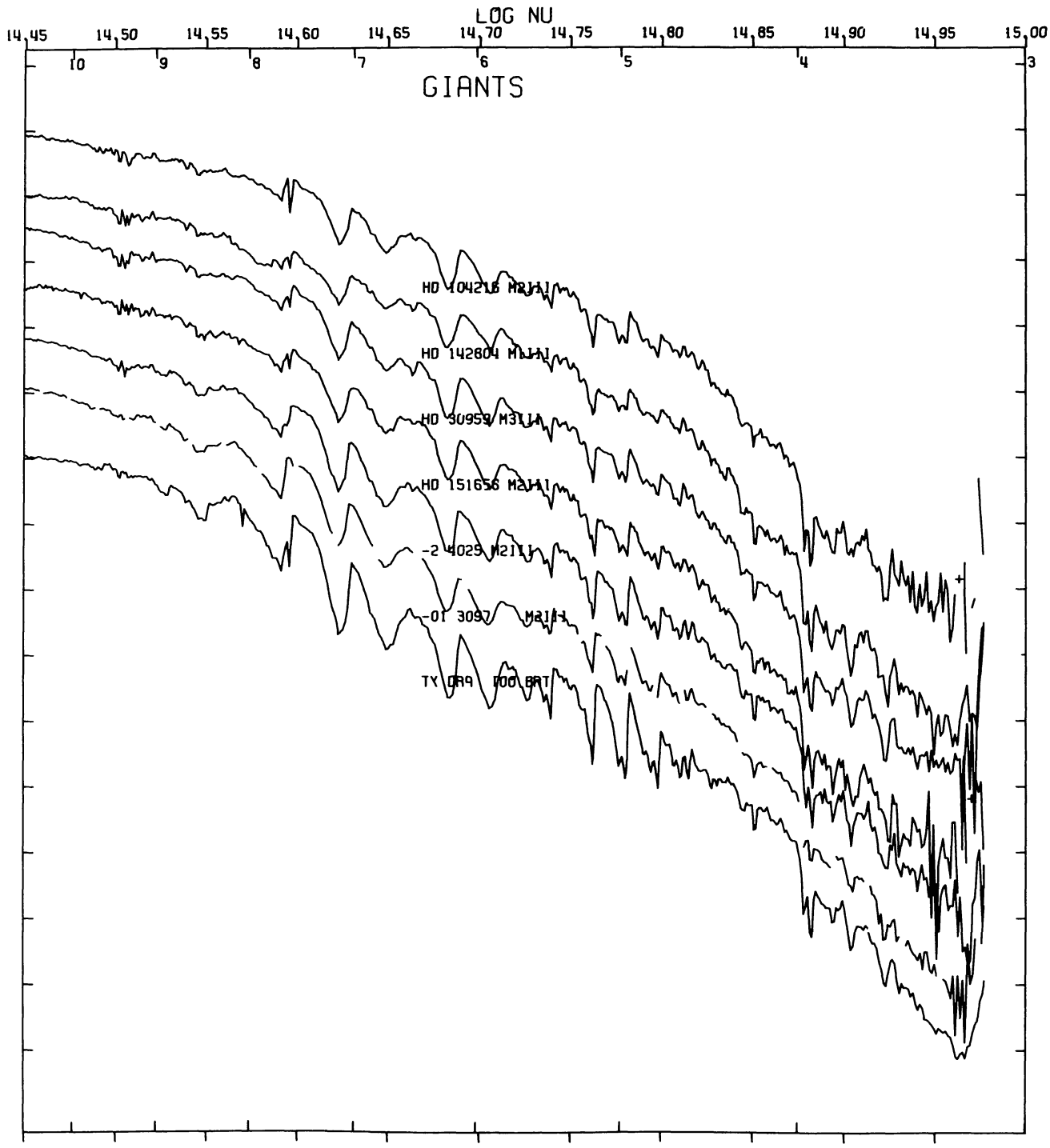

FIG. 2*p*.—Giants M1–M3

© American Astronomical Society • Provided by the NASA Astrophysics Data System

1983ApJS...52..121G

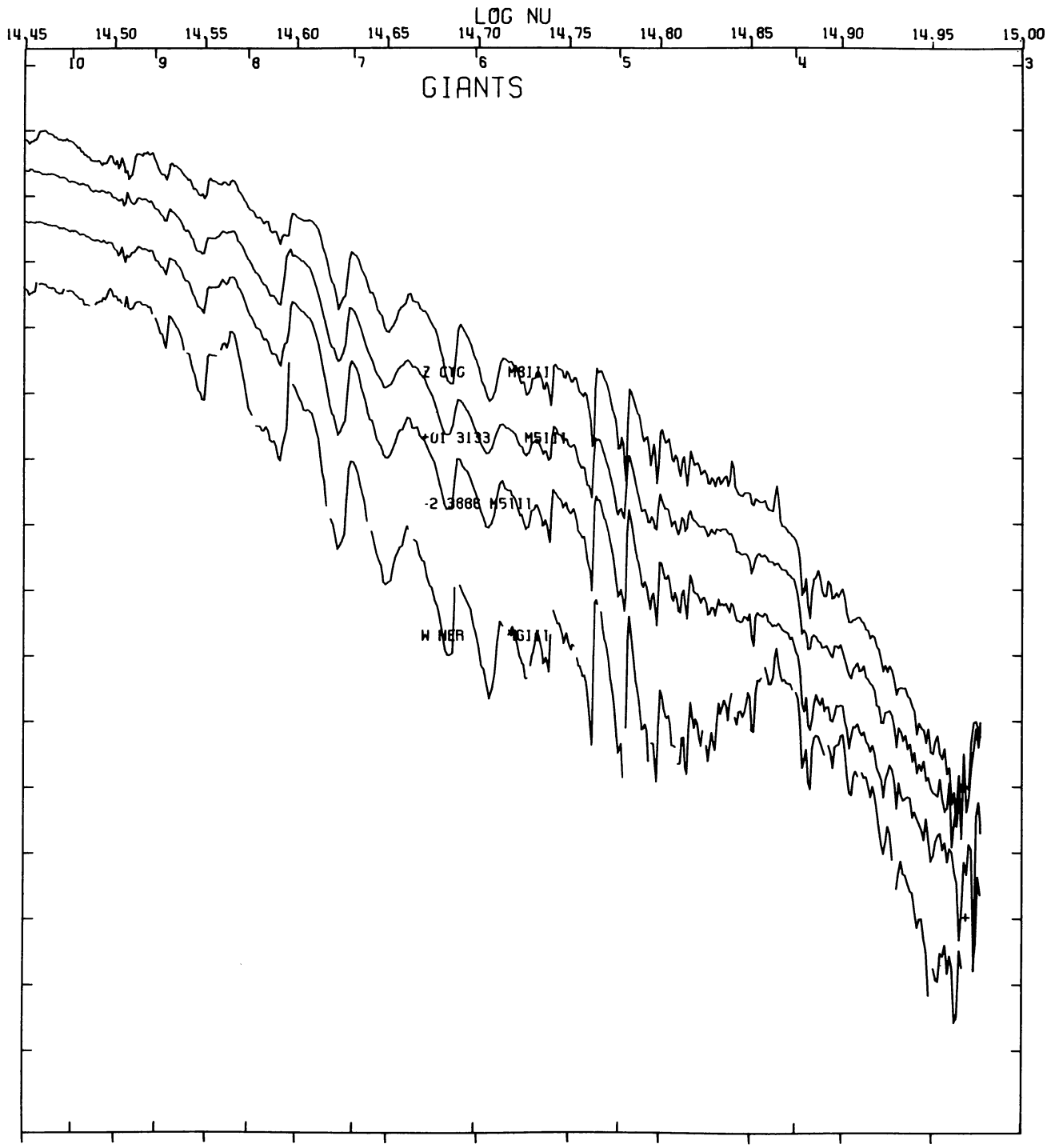

FIG. 2*q*.—Giants M5–M6

© American Astronomical Society • Provided by the NASA Astrophysics Data System

1983ApJS...52..121G

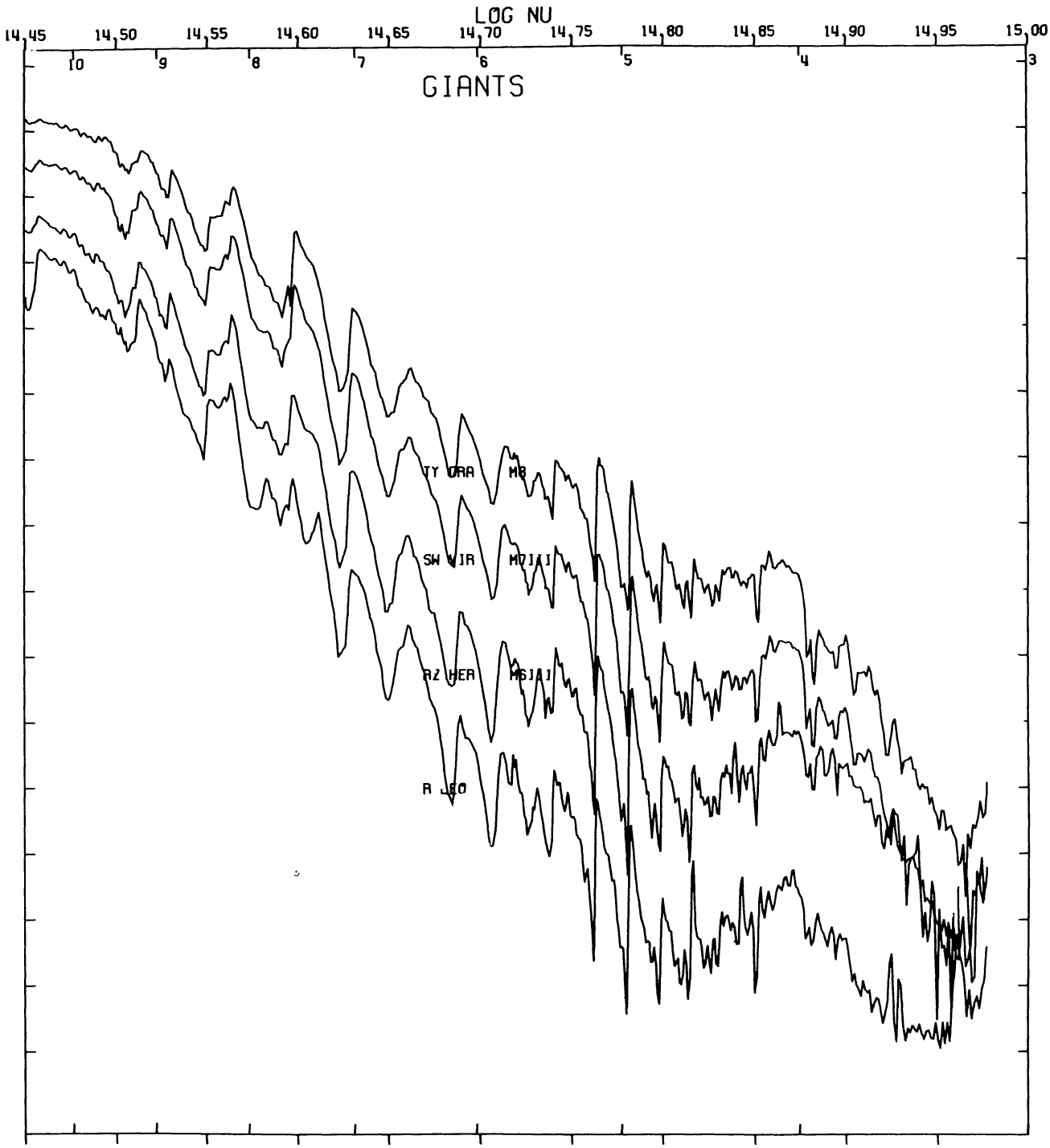

FIG. 2*r*.—Giants M6–M8; R Leo

© American Astronomical Society • Provided by the NASA Astrophysics Data System

1983ApJS...52..121G

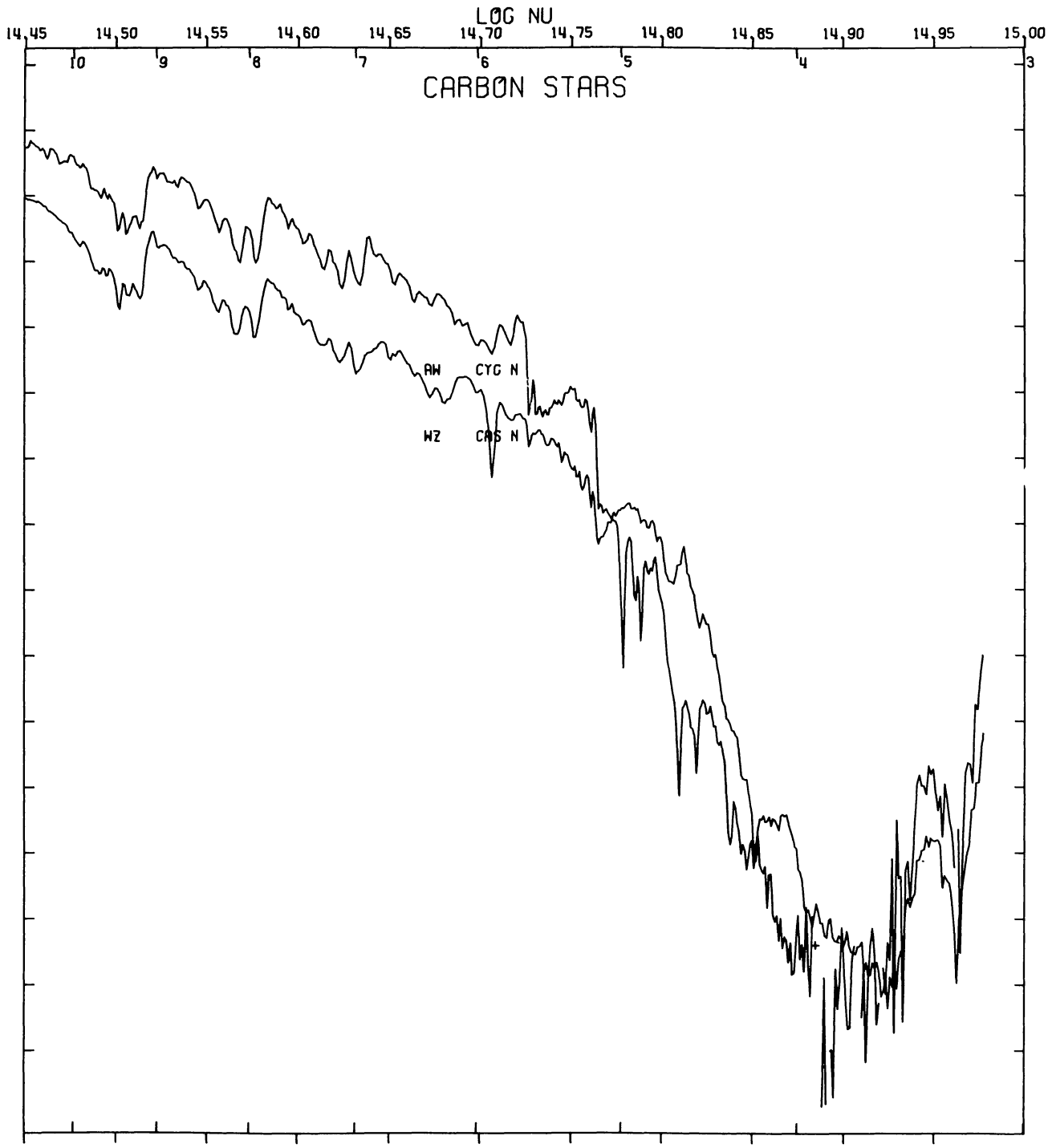

FIG. 2*s*.—Carbon stars

© American Astronomical Society • Provided by the NASA Astrophysics Data System

1983ApJS...52..121G

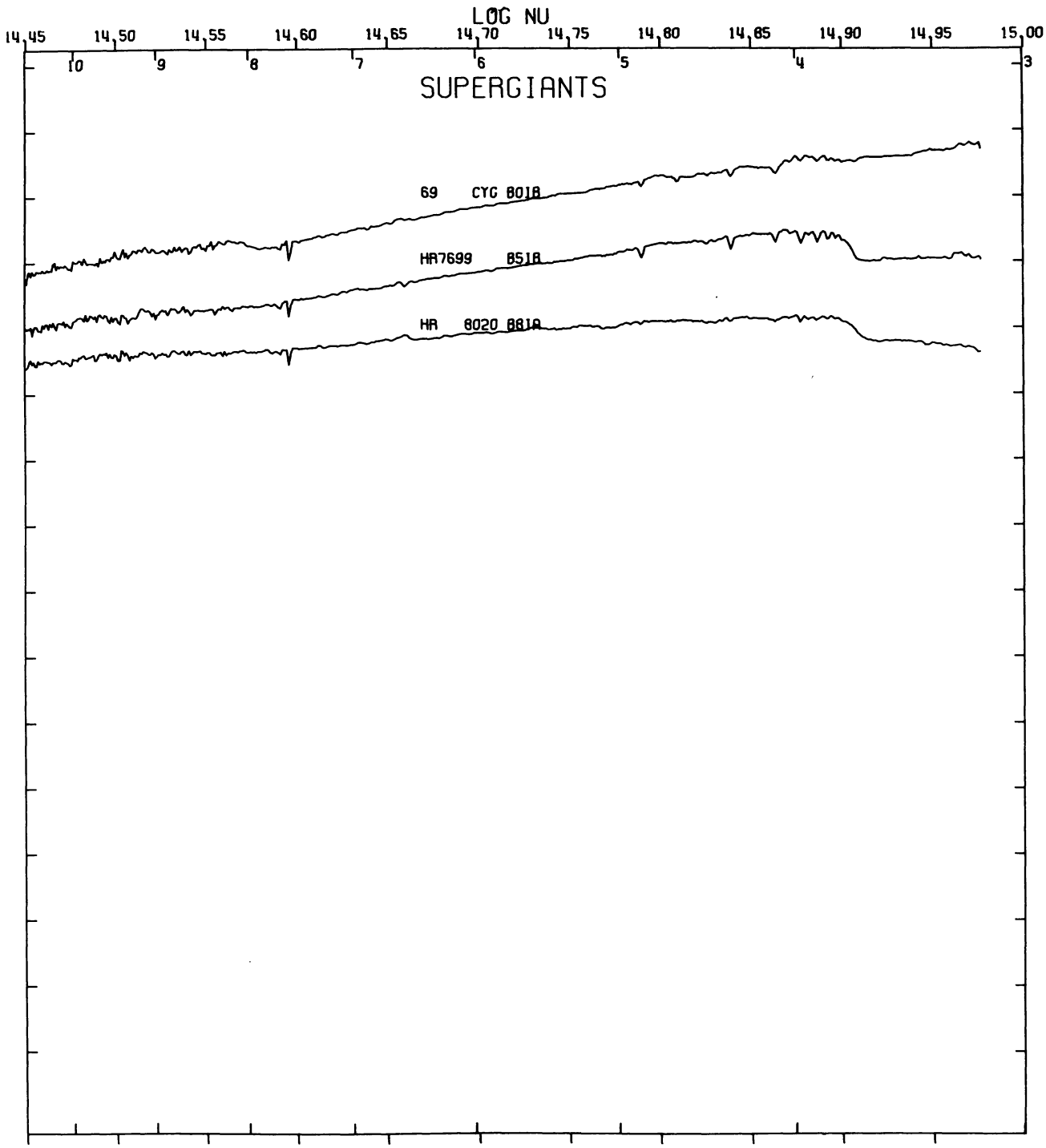

FIG. 2*t*.—Supergiants

© American Astronomical Society • Provided by the NASA Astrophysics Data System

1983ApJS...52..121G

APPENDIX

To allow the user to return the scans to their condition before any (de)reddening law was applied, we give the following formulae and algorithms that were used in the scan reductions. In this way the user can reverse our process and apply his/her own favorite laws.

At V we used

$$A_v = A * H * \csc b * \tan^{-1}(\sinh Z/H),$$

where

$$A = 0.7 \text{ m kpc}^{-1} \text{ and } H = 70 \text{ pc}.$$

At the other wavelengths we used Whitford's (1958) relation in the form of a Fortran function:

```
      FUNCTION ABSORP(WAVE)
      ABSORP = 0.0
      IF(WAVE.LE.900. .OR. WAVE.GT.2.E4) RETURN
      F = 1.E4/WAVE + 0.1
         DO1 K = 1,2
         E1 = -0.28 + 0.725 * F
         E2 = 0.40 + 0.42 * F
         A = E1
         IF(E2.LT.E1)A = E2
         ABSORP = 0.5 * A + ABSORP
    1    F = F - 0.2
      RETURN
      END
```

The function returned by ABSORP is A_λ. Fluxes are then dereddened by the small amount

$$\text{Flux}_\lambda(\text{dered}) = \text{Flux}_\lambda(\text{red}) * \text{dex}(0.4 * A_v * A_\lambda).$$

REFERENCES

Allen, C. W. 1973, *Astrophysical Quantities* (London: Athlone).
Ardeberg, A., and Virdefors, B. 1980, *Astr. Ap. Suppl.*, **40**, 307.
Blaauw, A. 1963, in *Stars and Stellar Systems*, Vol. **3**, *Basic Astronomical Data*, ed. K. Aa. Strand (Chicago: University of Chicago Press), p. 383.
Blanco, V. M., Demers, S., Douglass, G. G., and Fitzgerald, M. P. 1970, *Pub. US Naval Obs.*, **21**, 1.
Breger, M. 1974, *Ap. J.*, **192**, 75.
_____. 1976, *Ap. J. Suppl.*, **32**, 1.
Crawford, D. L., and Barnes, J. V. 1970, *A.J.*, **75**, 978.
Eggen, O. J. 1967, *Ap. J.*, **14**, 307.
_____. 1969, *Pub. A.S.P.*, **81**, 553.
_____. 1971*a*, *Ap. J.*, **165**, 317.
_____. 1971*b*, *Pub. A.S.P.*, **83**, 251.
Faber, S. M. 1977, in *The Evolution of Galaxies and Stellar Populations*, ed. B. M. Tinsley and R. B. Larson (New Haven: Yale University Observatory), p. 157.
Gunn, J. E., Stryker, L. L., and Tinsley, B. M. 1981, *Ap. J.*, **249**, 48.
Hauck, B., and Mermilliod, M. 1980, *Astr. Ap. Suppl.*, **40**, 1.
Hayes, D. S., and Latham, D. W. 1975, *Ap. J.*, **197**, 593.
Johnson, H. L. 1965, *Comm. Lunar and Planet. Lab.*, **3**, 79.
Kukarkin, B. V., and Parenago, P. P. 1954, *Trudy Shternberg Astr. Inst.*, **25**, 1.
Matthews, T. A., and Sandage, A. R. 1963, *Ap. J.*, **138**, 30.
Nicolet, B. 1978, *Astr. Ap. Suppl.*, **34**, 1.
Oke, J. B. 1964, *Ap. J.*, **140**, 689.
_____. 1969, *Pub. A.S.P.*, **81**, 11.
Oke, J. B., and Gunn, J. E. 1983, *Ap. J.*, **266**, 713.
Oke, J. B., and Schild, R. E. 1970, *Ap. J.*, **161**, 1015.
Sandage, A. R., and Smith, L. L. 1961, *Ap. J.*, **137**, 1057.
Serkowski, K. 1970, *Pub. A.S.P.*, **82**, 908.
Spinrad, H., and Taylor, B. J. 1969, *Ap. J.*, **157**, 1279.
Whitford, A. E. 1958, *A.J.*, **63**, 201.

Note added in proof.—Star 65 should read "HD 132683." Star 115 should read "HD 113493."

JAMES E. GUNN: Astrophysical Sciences, Peyton Hall, Princeton University, Princeton, NJ 08544

L. L. STRYKER: Dominion Astrophysical Observatory, 5071 W. Saanich Road, Victoria, B.C. V8X 4M6, Canada

© American Astronomical Society • Provided by the NASA Astrophysics Data System